1 **Reactive species formed upon interaction of water with fine particulate matter**

2 **from remote forest and polluted urban air**

3 Haijie Tong[1*], Fobang Liu[1,2], Alexander Filippi[1], Jake Wilson[1], Andrea M. Arangio[1,3], Yun Zhang[4],

4 Siyao Yue[5,6,7], Steven Lelieveld[1], Fangxia Shen[1,8], Helmi-Marja K. Keskinen[9,10], Jing Li[11],

5 Haoxuan Chen[11], Ting Zhang[11], Thorsten Hoffmann[4], Pingqing Fu[7], William H. Brune[12], Tuukka

6 Petäjä[9], Markku Kulmala[9], Maosheng Yao[11], Thomas Berkemeier[1], Manabu Shiraiwa[13], Ulrich

7 Pöschl[1]

8 [1] Multiphase Chemistry Department, Max Planck Institute for Chemistry, 55128 Mainz, Germany

9 [2] School of Chemical and Biomolecular Engineering, Georgia Institute of Technology, Atlanta, Georgia

10   30332, USA

11 [3] École polytechnique fédérale de Lausanne, Lausanne 1015, Switzerland

12 [4] Institute of Inorganic and Analytical Chemistry, Johannes Gutenberg University, 55128 Mainz, Germany

13 [5] State Key Laboratory of Atmospheric Boundary Layer Physics and Atmospheric Chemistry, Institute of

14   Atmospheric Physics, Chinese Academy of Sciences, Beijing, 100029, China

15 [6] College of Earth and Planetary Sciences, University of Chinese Academy of Sciences, Beijing, 100049,

16   China

17 [7] Institute of Surface-Earth System Science, Tianjin University, Tianjin, 300072, China

18 [8] School of Space and Environment, Beihang University, Beijing, 100191, China

19 [9] Institute for Atmospheric and Earth System Research / Physics, Faculty of Science, University of Helsinki,

20   P.O. Box 64, FIN-00014, Helsinki, Finland

21 [10] Hyytiälä Forestry Field Station, Hyytiäläntie 124, FI-35500 Korkeakoski, Finland

22 [11] College of Environmental Sciences and Engineering, Peking University, Beijing, 100871, China

23 [12] Department of Meteorology, Pennsylvania State University, University Park, Pennsylvania 16802, United

24   States

25 [13] Department of Chemistry, University of California, Irvine, California 92697-2025, USA

26 *Correspondence to: Haijie Tong (h.tong@mpic.de)

Atmospheric
Chemistry
and Physics
Discussions

27   **Abstract**

28   Interaction of water with fine particulate matter leads to the formation of reactive species (RS) that may

29   influence the aging, properties, and health effects of atmospheric aerosols. In this study, we explore the RS

30   yields of fine PM from remote forest (Hyytiälä, Finland) and polluted urban air (Mainz, Germany and

31   Beijing, China) and relate these yields to different chemical constituents and reaction mechanisms.

32   Ultrahigh-resolution mass spectrometry was used to characterize organic aerosol composition, electron

33   paramagnetic resonance (EPR) spectroscopy with a spin-trapping technique was used to determine the

34   concentrations $^{\bullet}OH$, $O_2^{\bullet-}$, and carbon- or oxygen-centered organic radicals, and a fluorometric assay was

35   used to quantify H_2O_2 concentration. The mass-specific yields of radicals were lower for sampling sites

36   with higher concentration of ambient $PM_{2.5}$ (particles with a diameter < 2.5 μm), whereas the H_2O_2 yields

37   exhibited no clear trend. The abundances of water-soluble transition metals and aromatics in ambient $PM_{2.5}$

38   were positively correlated with the relative fraction of $^{\bullet}OH$ to the totally detected radicals, but negatively

39   correlated with the relative fraction of carbon-centered radicals. Moreover, we found that the relative

40   fractions of different types of radicals formed by ambient $PM_{2.5}$ were comparable to the surrogate mixtures

41   comprising transition metals, organic hydroperoxide, H_2O_2, and humic or fulvic acids. Therein humic and

42   fulvic acids exhibited strong radical scavenging effect to substantially decrease the radical yield of mixtures

43   comprising cumene hydroperoxide and Fe^{2+}. The interplay of transition metals (e.g., iron), highly oxidized

44   compounds (e.g., organic hydroperoxides), and complexing agents (e.g., humic or fulvic acids), leads to

45   non-linear concentration dependencies of production and yields of different types of RS. Our findings show

46   that how the composition of $PM_{2.5}$ influences the amount and nature of RS produced upon interaction with

47   water, which may explain differences in the chemical reactivity and health effects of particulate matter in

48   clean and polluted air.

1 Introduction

Atmospheric fine particulate matter with a particle diameter < 2.5 µm ($PM_{2.5}$) forms reactive species (RS) upon interaction with water and respiratory antioxidants (Bates et al., 2015;Lakey et al., 2016;Park et al., 2018;Li et al., 2018;Tong et al., 2019). The umbrella term RS comprises reactive oxygen species (e.g., $^{\bullet}OH$, $O_2^{\bullet-}$, $^1O_2$, H_2O_2, and ROOH) as well as C- and O-centered organic radicals (Halliwell and Whiteman, 2004;Sies et al., 2017), which influence the chemical aging of atmospheric aerosols and their interaction with the biosphere (Pöschl and Shiraiwa, 2015;Reinmuth-Selzle et al., 2017;Shiraiwa et al., 2017). For example, Fenton-like reactions of hydroperoxides with transition metal ions contribute to the formation of aqueous-phase radicals including $^{\bullet}OH$ (Jacob, 2000;Enami et al., 2014;Anglada et al., 2015;Tong et al., 2016a), enhancing the conversion of organic precursors to secondary organic aerosols (SOA) (Donaldson and Valsaraj, 2010;Ervens et al., 2011;Gligorovski et al., 2015;Gilardoni et al., 2016). Moreover, $PM_{2.5}$ may generate excess concentrations of RS in human airways, causing antioxidant depletion, oxidative stress, and respiratory diseases (Nel, 2005;Cui et al., 2015;Lakey et al., 2016;Qu et al., 2017;Lelieveld and Pöschl, 2017;Rao et al., 2018).

The formation pathways and yields of RS from ambient PM and laboratory-generated SOA have been investigated in a wide range of studies (Valavanidis et al., 2005;Ohyama et al., 2007;Chen et al., 2010;Wang et al., 2011a;Wang et al., 2011b;Verma et al., 2014;Badali et al., 2015;Bates et al., 2015;Verma et al., 2015;Arangio et al., 2016;Tong et al., 2016a;Kuang et al., 2017;Tong et al., 2017;Zhou et al., 2018;Tong et al., 2019;Chowdhury et al., 2019;Fang et al., 2019;Liu et al., 2020). The mass, surface area, and chemical composition of PM were discussed as key factors influencing the reactivity of atmospheric aerosols (Møller et al., 2010;Fang et al., 2015;Jin et al., 2019). Among the substance groups associated with RS formation by PM in water are black carbon (Baumgartner et al., 2014), transition metals (Yu et al., 2018), oxidized aromatic compounds including quinones and environmentally persistent free radicals (Xia et al., 2004;Gehling et al., 2014;Charrier et al., 2014;Xiong et al., 2017), humic-like substances (Lin and Yu, 2011;Page et al., 2012;Fang et al., 2019), and peroxide-containing highly oxygenated organic molecules

74   (HOMs) (Chen et al., 2010;Wang et al., 2011b;Tong et al., 2016a;Tong et al., 2018;Tong et al., 2019;Fang

75   et al., 2020;Qiu et al., 2020). Moreover, the humic-like substances and other multifunctional compounds

76   containing carboxyl, carboxylate, phenolic, and quinoid groups may influence the redox activity of PM via

77   chelating transition metals (Laglera and van den Berg, 2009;Kostić et al., 2011;Catrouillet et al.,

78   2014;Gonzalez et al., 2017;Wang et al., 2018c;Win et al., 2018;Wei et al., 2019).

79   To assess the oxidative potential of ambient PM, the following cellular or acellular assays have been

80   used: dichloro-dihydro-fluorescein diacetate (DCFH-DA), dithiothreitol (DTT), ascorbic acid (AA),

81   macrophage, electron paramagnetic resonance (EPR), and surrogate lung fluids (SLF) (Landreman et al.,

82   2008;Charrier and Anastasio, 2012;Kalyanaraman et al., 2012;Charrier et al., 2014;Charrier and Anastasio,

83   2015;Fang et al., 2016;Tong et al., 2018;Bates et al., 2019;Fang et al., 2019;Molina et al., 2020;Crobeddu

84   et al., 2020). However, the interplay of different PM constituents often results in non-additive

85   characteristics of the RS yields or oxidative potential of PM (Charrier et al., 2014;Lakey et al., 2016;Wang

86   et al., 2018b). Thus, unraveling the adverse health effects of ambient PM requires systematic investigations

87   of the RS formation and chemical reactivity of PM from different sources and environments (Shiraiwa et

88   al., 2017).

89   The concentration of $PM_{2.5}$ and the composition of airborne organic matter vary considerably from clean

90   forest to polluted urban environments. For example, the $PM_{2.5}$ concentrations at the Hyytiälä forest site are

91   typically below 10 µg m^{-3}, with organic matter accounting for ~70% (Laakso et al., 2003;Maenhaut et al.,

92   2011), whereas the $PM_{2.5}$ concentrations in Beijing during winter can reach and exceed daily average values

93   of 150 µg m^{-3}, with organic matter accounting for ~40% (Huang et al., 2014). Moreover, anthropogenic

94   emissions can enhance the formation of biogenic SOA and HOM as well as the levels of particulate

95   transition metals, humic-like substances, and PM oxidative potential (Goldstein et al., 2009;Hoyle et al.,

96   2011;Liu et al., 2014;Xu et al., 2015;Ma et al., 2018;Pye et al., 2019;Shrivastava et al., 2019).

97   In this study, we compared the RS yields of $PM_{2.5}$ in clean and polluted environments. We used three

98   approaches to explore the RS formation by $PM_{2.5}$ from remote forest of Hyytiälä (Finland), intermediately

99   polluted city of Mainz (Germany), and heavily polluted megacity of Beijing (China) (Figure 1). To quantify

Atmospheric
Chemistry
and Physics
Discussions
Open Access
EGU

100   the abundances of redox-active PM constituents related to RS formation, we collected ambient $PM_{2.5}$ and

101   measured the chemical composition of organic matter, the abundance of water-soluble transition metals,

102   and the yield of radicals and H_2O_2 in the liquid phase (Figure 1a). To assess the influence of anthropogenic-

103   biogenic organic matter interactions on the RS formation by ambient $PM_{2.5}$, we analyzed the radical yield

104   of SOA generated by oxidation of mixed anthropogenic and biogenic precursors in a laboratory chamber

105   (Figure 1b). To get insights into the radical formation mechanism of ambient $PM_{2.5}$ in water, we

106   differentiated the influence of transition metals, organic hydroperoxide (ROOH), water-soluble humic acid

107   (HA) and fulvic acid (FA) on the radical formation by Fenton-like reactions (Figure 1c).

108   **2 Materials and methods**

109   **2.1 Chemicals**

110   The following chemicals were used as received without further purification: β-pinene (99%, Sigma-

111   Aldrich), naphthalene (99.6%, Alfa Aesar GmbH&Co KG), cumene hydroperoxide (80%, Sigma-Aldrich),

112   H_2O_2 (30%, Sigma-Aldrich), $FeSO_4 \cdot 7H_2O$ (F7002, Sigma-Aldrich), $CuSO_4 \cdot 5H_2O$ (209198, Sigma-

113   Aldrich), $NiCl_2$ (98%, Sigma-Aldrich), $MnCl_2$ (≥99%, Sigma-Aldrich), VCl_2 (85%, Sigma-Aldrich), NaCl

114   (443824T, VWR International GmbH), KH_2PO_4 (≥99%, Alfa Aesar GmbH&Co KG), Na_2HPO_4 (≥99.999%,

115   Fluka), humic acid (53680, Sigma-Aldrich), fulvic acid (AG-CN2-0135-M005, Adipogen), 5-tert-

116   Butoxycarbonyl-5-methyl-1-pyrroline-N-oxide (BMPO, high purity, Enzo Life Sciences, Inc.), H_2O_2 assay

117   kit (MAK165, Sigma-Aldrich), ultra-pure water (14211-1L-F, Sigma-Aldrich), 47 mm diameter Teflon

118   filters (JVWP04700, Omnipore membrane filter), and micropipettes (50 μL, Brand GmbH&Co KG). The

119   used neutral saline (pH=7.4) consists of 10 mM phosphate buffer (2.2 mM KH_2PO_4 and 7.8 mM Na_2HPO_4)

120   and 114 mM NaCl, which was used to simulate physiologically relevant condition.

121   **2.2 Collection and extraction of ambient fine PM**

122   Ambient fine particles were collected onto Teflon filters for all sites. The Hyytiälä $PM_{2.5}$ was collected

123   using a three-stage cascade impactor (Dekati® PM10) at the Station for Measuring Forest Ecosystem-

124   Atmosphere Relations station (SMEAR II station, Finland) during 31 May-19 July 2017 (Hari and Kulmala,

125   2005). The Mainz fine PM was collected using a micro-orifice uniform deposit impactor (MOUDI, 122-R,

126   MSP Corporation) (Arangio et al., 2016) on the roof of Max Planck Institute for Chemistry during 22

127   August-17 November 2017 and 23-31 August 2018. The Beijing winter $PM_{2.5}$ was collected using a 4-

128   channel $PM_{2.5}$ air sampler (TH-16, Wuhan Tianhong Instruments Co., Ltd.) in the campus of the Peking

129   University, an urban site of Beijing, during 20 December-13 January 2016 and 6 November-17 January

130   2018 (Lin et al., 2015). The sampling time for a single filter sample in Hyytiälä, Mainz, and Beijing are 48-

131   72, 25-54, and 5-24 h, respectively, depending on the local PM concentrations. More information about the

132   sampling sites and instrumentation is shown in Table S1. After sampling, all filter samples were put in petri

133   dishes and stored in a -80 ℃ freezer before analysis. To determine the mass of collected PM, each filter

134   was weighed before and after the collection using a high sensitivity balance (±10 µg, Mettler Toledo

135   XSE105DU). In Hyytiälä, the PM_1 and $PM_{1-2.5}$ were separately sampled, which were combined and

136   extracted together to represent $PM_{2.5}$ samples. Mainz PM with cut-size range of 0.056-1.8 µm is taken as a

137   proxy for $PM_{2.5}$. Particle concentrations in aqueous extracts were estimated to be in the range of 200-6000

138    $\mu g \ mL^{-1}$ (Figure S1).

2.3 Formation, collection, and extraction of laboratory-generated SOA

140   To generate SOA from mixed anthropogenic and biogenic precursors, different concentrations of gas-phase

141   naphthalene and β-pinene were mixed and oxidized in a potential aerosol mass (PAM) chamber, i.e., an

142   oxidation flow reactor (OFR) (Kang et al., 2007;Tong et al., 2018). Naphthalene and β-pinene were used

143   as representative SOA precursors in Beijing and Hyytiälä, respectively (Hakola et al., 2012;Huang et al.,

144   2019). The concentrations of gas-phase O_3 and $^{\bullet}OH$ in the PAM chamber were ~1 ppm and ~5.0×10^{11} cm-

145   ^{3}, respectively. SOA was produced by adjusting the relative concentrations of naphthalene to the sum of it

146   with β-pinene (i.e., [naphthalene]/([naphthalene] + [β-pinene])) to be ~9%, ~23%, and ~38%, respectively.

147   The concentrations of naphthalene and β-pinene were 0.2-0.6 ppm and 1.0-2.5 ppm, respectively, which

148   were determined on the basis of a calibration function measured by gas chromatography mass spectrometry

149   (Tong et al., 2018). To investigate the influece of ozone/β-pinene ratios on redox property of SOA, we

150   measured the aqueous phase radical yields of SOA particles formed from oxidation of ~1 ppm and ~2.5

151   ppm β-pinene with the same concentration of ozone. With a similar purpose, we measured the radial yields

152   of SOA formed from oxidation of ~0.2 ppm and ~0.6 ppm naphthalene by the same concenteation of gas-

153   phase OH radical. The mean radical yields of β-pinene and naphthalene SOA formed at different

154   concentrations of precursors are compared in Sect. 3.4. The number and size distributions of SOA particles

155   were meaured using a scanning mobility particle sizer (SMPS, GRIMM Aerosol Technik GmbH&Co. KG).

156   When the SOA concentration is stable, 47 mm diameter Teflon filters (JVWP04700, Omnipore membrane

157   filter) were used to collect SOA particles, which were extracted into water solutions within 2 minutes after

158   the sampling. More information about the SOA formation, characterization, collection, and extraction can

159   be found in previous studies (Tong et al., 2016a;Tong et al., 2017;Tong et al., 2018;Tong et al., 2019).

160   **2.4 Surrogate mixtures**

161   Considering that cumene hydroperoxide (CHP), humic acid (HA), and fulvic acid (FA) have been used as

162   model compounds mimicking the redox-active substances in biogenic and anthropogenic PM (Lin and Yu,

163   2011;Ma et al., 2018;Tong et al., 2019), we measured the relative fractions (RF) of different radicals formed

164   by surrogate mixtures of $CHP+Fe^{2+}+Cu^{2+}+HA+H_2O_2$ to simulate the radical formation by fine PM from

165   Hyytiälä, Mainz, and Beijing. The H_2O_2 was treated as a redox-active constituent preexisting in PM samples

166   before extraction. The following method was used to make HA or FA solutions. First, 0-1000 µg mL^{-1} HA

167   or FA water suspensions were made. Then, the suspensions were sonicated for 3 minutes to accelerate the

168   dissolution of HA or FA. Afterwards, the sonicated suspensions were centrifuged at 6000 rpm (MiniStar,

169   VWR International bvba) for 2 minutes. Finally, the supernatants were taken out from the centrifuge tubes

170   with pipettes and stored in glass vials under 4-8 °C condition before analysis. The HA or FA solutions were

171   prepared freshly day-to-day. To determine the concentrations of dissolved HA or FA, aliquots of the

172   supernatants were dried with pure N_2 flow (1-2 bar) and weighted with a high sensitivity balance (± 0.01

173   mg, Mettler Toledo XSE105DU). The concentrations of Fe^{2+}, Cu^{2+}, HA, and H_2O_2 in the surrogate mixtures

174   are 43 µM, 3 µM, 4 mg L^{-1}, and 7 µM, which are based on the measurement of ambient PM extracts (Fe^{2+}

175   and Cu^{2+}, Section 2.8) or the estimated abundance in ambient PM (CHP, HA, FA, and H_2O_2, SI). To explore

Atmospheric
Chemistry
and Physics
Discussions

Open Access

EGU

176   the influence of HA/FA on Fenton-like reactions, the radical formation in the following aqueous mixtures

177   was also analyzed: CHP+Fe^{2+}, CHP+Cu^{2+}, CHP+Cu^{2+}+HA, CHP+Cu^{2+}+FA. The concentrations of Fe^{2+},

178   Cu^{2+}, HA, FA, and H_2O_2 in these solutions are 15-300 µM, 15-300 µM, 0-180 µg mL^{-1}, 0-180 µg mL^{-1}, 0-

179   300 µM, respectively.

180   **2.5 Quantification of radicals by EPR**

181   5-tert-Butoxycarbonyl-5-methyl-1-pyrroline-N-oxide (BMPO) was used as a spin-trapping agent for

182   detecting different types of radicals formed in the extracts of PM. Ambient PM or laboratory-generated

183   SOA were extracted from Teflon filters into 10 mM BMPO neutral saline or water solutions by vortex

184   shaking for ~15 minutes (with Heidolph Reax 1). Around one fourth of each ambient PM filter or a whole

185   SOA-loaded filter was used for extraction. It was assumed that during the extraction process, most of the

186   short-lived radicals have reacted with BMPO to form stable adducts.

187   A continuous-wave electron paramagnetic resonance (CW-EPR) X-band spectrometer (EMXplus-10/12;

188   Bruker Corporation) was applied for the identification and quantification of radical adducts (Tong et al.,

189   2016a;Tong et al., 2017;Tong et al., 2018;Tong et al., 2019). In order to increase the signal to noise ratio

190   of EPR spectra, some of the extracts were concentrated by a factor of 5 - 20 through 15 - 20 minutes drying

191   under 1-2 bar pure N_2 flow. The EPR spectra of BMPO-radical adducts were recorded by setting the

192   following operating parameters: a microwave frequency of 9.84 GHz, a microwave power of 0.017 mW

193   (20 dB), a receiver gain of 40 dB, a modulation amplitude of 1 G, a scan number of 50, a sweep width of

194   100 G, a modulation frequency of 100 kHz, a conversion time of 11 ms, and a time constant of 10 ms.

195   To average EPR spectra of different $PM_{2.5}$ extracts for each site, the magnetic field values of each

196   spectrum was transformed to g-values. Then we used the Bruker software, Xenon to do the averaging,

197   irrespective of the concentrations of $PM_{2.5}$ in extracts. The spin-counting method embedded in Xenon was

198   applied to quantify radical adducts. The spin-counting method was calibrated using the standard compound

199   4-hydroxy-2,2,6,6-tetramethylpiperidin-1-oxyl (TEMPOL). To obtain the relative yields of $^{\bullet}OH$, $O_2^{\bullet-}$, C-

200   and O-centered organic radicals, EPR spectra were simulated and fitted using the Xenon software before

201 deconvolution (Arangio et al., 2016;Tong et al., 2018). The weight of assigned species accounts on average

202 for more than 95% of totally observed radical adducts, which is characterized by the peak area ratios of

203 corresponding species. EPR spectra with low signal-to-noise ratio introduce uncertainty into the parameters

204 describing the lineshape of peaks representing radical adducts (Tseitlin et al., 2012), causing a total

205 quantification uncertainty of 0-19% for the weight and total concentrations of different radical species. The

206 hyperfine coupling constants used for spectrum fitting are shown in Table S2. More information on the

207 hyperfine coupling constants of different types of BMPO radical adducts can be found in previous studies

208 (Zhao et al., 2001;Arangio et al., 2016).

209 **2.6 Measurement of H_2O_2 yields**

210 We extracted ambient $PM_{2.5}$ from one fourth of each Teflon filter into 1 mL ultra-pure water or neutral

211 saline by stirring it with a vortex shaker for ~15 minutes. Afterwards, the extracts were centrifuged at 9000

212 rpm (Eppendorf Minispin) for 3 minutes to remove the insoluble particles. Finally, the concentration of

213 H_2O_2 in the supernatant was measured using the MAK165 assay kit (Yan et al., 2017;Tong et al., 2018). 50

214 µL of supernatant and 50 µL of a Master Mix solution containing horseradish peroxidase and Amplex Red

215 substrate were mixed in a 96-well plate. The horseradish peroxidase catalyzed the oxidation of Amplex Red

216 by H_2O_2 to form fluorescent resorufin (Wang et al., 2017), which was consequently quantified using a

217 microplate reader (Synergy™ NEO, BioTek, excitation at 540 nm and emission at 590 nm) after 30 minutes

218 of incubation. The concentration of H_2O_2 in aqueous PM extracts was determined using an H_2O_2 calibration

219 curve based on standard H_2O_2 solutions and also corrected by blank measurements (Tong et al., 2018).

220 **2.7 Mass spectrometry of organic compounds**

221 By using a Q-Exactive Orbitrap mass spectrometer (Thermo Fisher Scientific, MA, USA) coupled with an

222 ultra-high performance liquid chromatography (UHPLC) system (Dionex UltiMate 3000, Thermo

223 Scientific, Germany) (Wang et al., 2018a;Wang et al., 2019;Tong et al., 2019), we characterized the HOMs

224 and aromatic compounds in Hyytiälä, Mainz, and Beijing winter fine PM samples in negative ionization

225 mode. We processed the MS spectrum and UHPLC chromatogram of measured samples through a non-

226   target screening approach by using the commercially available software SIEVE® (Thermo Fisher Scientific,

227   MA, USA). Then, we blank-corrected the signals with peak intensity $> 1 \times 10^5$. Afterwards, we used the

228   following criteria to assign molecular formulae and filter out the irrational ones: (a) the number of atoms

229   of C, H, O, N, S, and Cl should be in the range of 1-39, 1-72, 0-20, 0-7, 0-4, and 0-2. (b) Atomic ratios of

230   H/C, O/C, N/C, S/C, and Cl/C should be in the range of 0.3-3, 0-3, 0-1.3, 0-0.8, and 0-0.8, respectively.

231   The HOMs are defined as formulae fell into the following chemical composition range of $C_xH_yO_z$:

232   monomers with x = 8–10, y = 12–16, z = 6–12, and z/x > 0.7; dimers with x = 17–20, y = 26–32 and z = 8–

233   18 (Ehn et al., 2014;Tröstl et al., 2016;Tong et al., 2019). Aromatics in this study are defined to be

234   compounds with aromaticity index (AI) > 0.5 and aromaticity equivalent (X_c) > 2.5, with the parameters

235   accounting for the fraction of oxygen and sulfur atoms involved in π-bond structures of a compound to be

236   set as 1 (Koch and Dittmar, 2006;Yassine et al., 2014;Tong et al., 2016b). Beyond this, The relative

237   abundance of HOMs or aromatic compounds is defined to be the sum chromatographic area of HOMs or

238   aromatics divided by the sum chromatographic area of all assigned organic compounds, with < 30% of

239   totally detected organic compounds not assigned (Wang et al., 2018a).

240   **2.8 Determination of water-soluble transition metal concentrations**

241   Based on the same extraction method as the H_2O_2 analysis in section 2.6, the concentration of five selected

242   water-soluble transition metal species (Fe, Cu, Mn, Ni and V) in the supernatants of $PM_{2.5}$ extracts was

243   quantified using an inductively coupled plasma mass spectrometer (ICP-MS, Agilent 7900). These five

244   transition metal species were chosen for analysis due to their prominent concentrations and higher oxidative

245   potential (Charrier and Anastasio, 2012). A calibration curve for the ICP-MS analysis was made by

246   measuring standard multi-element stock solutions (Custom Grade, Inorganic Ventures). An aliquot of the

247   supernatants was diluted and acidified using a mixture of nitric acid (5%) and hydrofluoric acid (1%), which

248   was finalized to be 5 mL before analysis. The measured transition metal concentrations were blank-

249   corrected and shown in corresponding figures. The detection limit of the ICP-MS analysis in this study was

250   typically < 40 ng L^{-1}. The $PM_{2.5}$ samples collected on 2 June, 7 June, 9 June, 12 June in 2017 in Hyytiälä,

251   on 22 August, 26 August, 28 August, 25 September, 25 October, 14 November in 2017 in Mainz, and all

252   the 12 $PM_{2.5}$ samples from Beijing winter were used for transition metal analysis. Temporal evolution of

253   water-soluble transition metal concentrations in water extracts of Mainz $PM_{2.5}$ were also measured, and we

254   found that the total ion concentration of Fe, Cu, Mn, Ni, and V showed a rapid rise during the first 15 min

255   (Figure S2a), but at a much slower rate afterwards (Figure S2b).

256   **3 Results and discussion**

257   **3.1 Relative yields of different types of radicals from ambient $PM_{2.5}$**

258   Figure 2a shows the averaged EPR spectra of BMPO-radical adducts in neutral saline extracts of $PM_{2.5}$

259   samples from Hyytiälä, Mainz (cut-size range 0.056-1.8 µm PM as a proxy), and Beijing. Each spectrum

260   is composed of multiple peaks attributable to different types of BMPO-radical adducts. The dotted vertical

261   lines with different colors indicate the peaks attributable to adducts of BMPO with $^{\bullet}OH$ (green), $O_2^{\bullet-}$

262   (orange), C- (blue) and O-centered organic radicals (purple) (Zhao et al., 2001;Arangio et al., 2016),

263   respectively. The spectrum of Hyytiälä $PM_{2.5}$ is dominated by peaks attributable to C-centered radicals. In

264   contrast, the spectrum of Mainz $PM_{2.5}$ comprises strong peaks attributable to $^{\bullet}OH$ and C-centered radicals,

265   with $^{\bullet}OH$ exhibiting stronger signals. Finally, the spectrum of Beijing winter $PM_{2.5}$ is mainly composed of

266   four peaks attributable to $^{\bullet}OH$.

267   Figure 2b shows the averaged relative fractions (RF) of $^{\bullet}OH$, $O_2^{\bullet-}$, C- and O-centered organic radicals

268   generated by multiple PM samples from each site. In line with visual inspection of the spectra in Figure 2a,

269   the $PM_{2.5}$ from clean forest site generates relatively more C- and O-centered organic radicals but less $^{\bullet}OH$,

270   vice versa for the radical yield by $PM_{2.5}$ from polluted areas. Specifically, the mean RF of C- and O-centered

271   organic radicals, ordered from highest to lowest are: Hyytiälä (66% and 11%) > Mainz (46% and 10%) >

272   Beijing (39% and 5%). Note that, the significantly higher RF of C-centered radicals than O-centered organic

273   radicals may be induced by the higher yield and stability of BMPO-C-centered radical adduct in the liquid

274   phase (De Araujo et al., 2006). Moreover, the C- and O-centered organic radicals may comprise a series of

275   radicals with different molecular structures, the yields of which are associated with aqueous redox

276   chemistry of organic matter such as Fenton-like reactions (Arangio et al., 2016;Tong et al., 2018;Tong et

277   al., 2019). The mean RF of $^{\bullet}OH$, ordered from lowest to highest are: 21% (Hyytiälä) < 38% (Mainz) < 53%

278   (Beijing). The presence of $^{\bullet}OH$ is related to multiple formation pathways, such as Fenton-like reactions,

279   thermal or hydrolytic decomposition of peroxide-containing HOMs, and redox chemistry of

280   environmentally persistent free radicals or aromatic compounds-containing humic-like substances

281   (Chevallier et al., 2004;Valavanidis et al., 2005;Li et al., 2008;Page et al., 2012;Gehling et al., 2014;Tong

282   et al., 2016a;Tong et al., 2017;Tong et al., 2018;Tong et al., 2019;Qiu et al., 2020). The mean RF of $O_2^{\bullet -}$

283   only varies slightly in the range of 2-6%, showing no clear trend and within the range of standard errors in

284   Figure 2b.

285   **3.2 Mass-specific and air sample volume-specific yields of RS from ambient PM$_{2.5}$**

286   Figure 3 shows the mass-specific and air sample volume-specific yields of reactive species (RS) including

287   radicals, H_2O_2, and the sum of radicals and H_2O_2 by PM$_{2.5}$ from Hyytiälä, Mainz, and Beijing. The mass-

288   specific yields of RS are shown in the unit of pmol µg^{-1} of PM$_{2.5}$, reflecting the redox activities of PM$_{2.5}$

289   irrespective of filter loadings. The air sample volume-specific yields of RS are shown in the unit of pmol

290   m^{-3} of air, indicating that the redox activities of PM$_{2.5}$ scale with atmospheric concentration of PM$_{2.5}$. We

291   note that, while the more polluted sampling sites led to higher mass loadings, the concentrations of PM in

292   extracts were found to have a tiny impact on the radical yields (Figure S1c and S1d).

293   Figure 3a shows that the mass-specific radical yields are negatively correlated with PM$_{2.5}$ mass

294   concentrations. The mean concentrations of PM$_{2.5}$ are lower to higher in the order of 5 (Hyytiälä) < 16

295   (Mainz) < 202 µg m^{-3} (Beijing), whereas the radical yields are in a reverse order of 0.58 > 0.33 > 0.07 pmol

296   µg^{-1}. The higher mass-specific radical yield of PM$_{2.5}$ from Hyytiälä may be associated with the higher

297   abundance of particulate organic matter, which includes quinones and organic hydroperoxides that undergo

298   thermal, photonic, or hydrolytical dissociation as well as redox chemistry such as Fenton-like reactions to

299   produce radicals (Badali et al., 2015;Tong et al., 2016a;Tong et al., 2019). More than 70% of PM$_{2.5}$ in

300   Hyytiälä forest is composed of organic matter (Jimenez et al., 2009;Maenhaut et al., 2011), whereas the

301   abundances of organic matter in Mainz autumn and Beijing winter PM$_{2.5}$ are ~40% (Jimenez et al.,

302   2009;Huang et al., 2014), which might in part explain the lower radical yield of these samples. Figure 3a

303   also shows that the mass-specific H_2O_2 yields of $PM_{2.5}$ from Hyytiälä (~2.2 pmol μg^{-1}), Mainz (~3.4 pmol

304   μg^{-1}), and Beijing (~3.4 pmol μg^{-1}) exhibit a weak positive correlation with $PM_{2.5}$ mass concentrations,

305   agreeing with previous measurements of the H_2O_2 formation by fine PM from different districts of Los

306   Angeles (Arellanes et al., 2006;Wang et al., 2012) (Figure S4a). The higher H_2O_2 yield of urban fine PM

307   may be associated with its higher abundance of transition metals and aromatic-containing organic matter

308   (e.g., quinones and humic-like substances), which have been found as redox-active constituents to produce

309   H_2O_2 upon dissolution of ambient PM or laboratory-generated SOA in water (Arellanes et al., 2006;Chung

310   et al., 2006;Wang et al., 2010;Wang et al., 2012). The weak correlation of mass-specific H_2O_2 yields and

311    $PM_{2.5}$ concentrations reflects the varying redox activity of $PM_{2.5}$ from different regions, which is driven by

312   the PM source-dependent composition, abundance, and chemistry of redox active substances (e.g.,

313   transition metals and organic matter).

314   Figures 3b and S4b show that the air sample volume-specific yields of total RS (H_2O_2+radicals) increase

315   as $PM_{2.5}$ concentrations increase, reflecting a higher RS formation in per cubic meter of polluted urban air.

316   Specifically, the relative air sample volume-specific yields of H_2O_2 (i.e., $[H_2O_2]/([H_2O_2]+[radicals])$),

317   ordered from lowest to highest are: 78% (Hyytiälä) > 91% (Mainz) > 97% (Beijing), whereas the relative

318   air sample volume-specific radical yields (i.e., $[radicals]/([H_2O_2]+[radicals])$) are in the reverse order of

319   22% > 9% > 3%. The relatively stable H_2O_2 becomes increasingly important for the reactivity of ambient

320    $PM_{2.5}$ compared to the more reactive radicals when transitioning from clean to polluted conditions. Due to

321   its stability, H_2O_2 has been found previously to dominate the concentrations of RS formed by $PM_{2.5}$ in liquid

322   phase with the presence of antioxidants but absence of spin traps (Lakey et al., 2016;Tong et al., 2018).

323   This study shows a time integral concentration rather than the RS concentration taking into account the

324   different lifetimes and evolution pathways of radicals and H_2O_2. H_2O_2 still constitutes the biggest fraction

325   of RS detected. Of note, the EPR method may not detect all radicals produced but rather a fraction that is

326   trapped with BMPO before undergoing other radical termination reactions. It is also notable that we

327   measured the RS yields of PM from three different areas. Further measurements of PM from more locations

13

328   may shift the trend of the RS yields in Figure 3 by a certain degree, the extent of which warranty follow-up

329   studies.

330   **3.3 Correlation of radical yield with chemical composition of ambient PM$_{2.5}$**

331   Figure 4 shows how the relative fractions (RF) of C-centered radicals and $^\bullet$OH in aqueous extracts of

332   ambient PM$_{2.5}$ are correlated with the abundance of HOMs, aromatic compounds, and water-soluble

333   transition metals. Figure 4a shows that the relative abundance of HOMs exhibits a positive correlation with

334   the RF of C-centered radicals, whereas a negative correlation with the RF of $^\bullet$OH. The relative abundance

335   of HOMs, ordered from lowest to highest are: ~0.2% (Beijing) < ~6% (Mainz) < ~10% (Hyytiälä) (Tong

336   et al., 2019), and the RF of C-centered radicals is in the same order of 39% < 46% < 66%, but the RF of

337     $^\bullet$OH are in the reverse order of 53% > 38% > 21%. The higher RF of C-centered radicals formed by PM$_{2.5}$

338   from less-polluted air is in the same trend as the total mass-specific radical yield of PM$_{2.5}$ from these sites

339   (Figure 3a), confirming previous results that peroxide-containing HOMs may play an important role in

340   organic radical formation (Tong et al., 2016a;Tong et al., 2019).

341   In contrast to HOMs, the relative abundance of aromatic compounds in PM$_{2.5}$ is higher in polluted urban

342   air compared to clean forest: ~0.2% (Hyytiälä) < ~2% (Mainz) < ~16% (Beijing) (Figure 4b), causing a

343   positive correlation with the RF of $^\bullet$OH, but a negative correlation with the RF of C-centered radicals. The

344   higher relative abundance of particulate aromatics in Beijing compared to Hyytiälä can be attributed to the

345   stronger anthropogenic emissions (e.g., from traffic) at the polluted urban site (Jimenez et al., 2009;Zhang

346   and Tao, 2009;Elser et al., 2016;An et al., 2019). The chemistry of oxygenated aromatic-containing

347   substances, such as quinones and semiquinones, may enhance the conversion of other RS (e.g., $O_2^{\bullet-}$) into

348     $^\bullet$OH due to redox cycling and interaction with water (Chung et al., 2006;Khachatryan et al., 2011;Fan et

349   al., 2016).

350   Similar to the aromatics, the transition metal abundances exhibit a positive correlation with the RF of

351     $^\bullet$OH, but a negative correlation with the RF of C-centered radicals (Figure 4c). The abundance of water-

352   soluble transition metals in PM$_{2.5}$ from different locations, ordered from lowest to highest are: 13.4

353   (Hyytiälä) < 19.6 (Mainz) < 27.8 (Beijing) pmol µg^{-1}, and the RF of $^\bullet$OH is in the same order of 21% < 38%

354   < 53%, whereas the relative fraction of C-centered radicals is in the reverse order of 66% > 46% > 39%.

355   The consistently higher abundance of water-soluble transition metals and RF of $^\bullet$OH of urban PM$_{2.5}$ may

356   reflect the importance of Fenton-like reactions in radical formation in polluted air, as H$_2$O$_2$ and

357   hydroperoxides can be efficiently converted into $^\bullet$OH. Moreover, several studies have reported that metal-

358   organic interactions may alter the oxidative potential and RS yield of PM under atmospheric and

359   physiological conditions (Zuo and Hoigne, 1992;Singh and Gupta, 2016;Cheng et al., 2017;Wang et al.,

360   2018b;Wei et al., 2019;Lin and Yu, 2020). Thus, investigations on the radical chemistry of transition metals

361   strongly benefit from determination of organic aerosols to illuminate the mechanism of RS formation.

362   Finally, additional measurements of PM$_{2.5}$ from more locations may shift the correlation of radical yields

363   and abundances of transition metals and organic matter by a certain degree, the extent of which also

364   warranty follow-up studies.

365   **3.4 Radical yield of laboratory-generated SOA**

366   To investigate the influence of biogenic-anthropogenic organic matter interaction on the formation of

367   aqueous radicals, we measured the radical yield of SOA generated from oxidation of mixed naphthalene

368   and β-pinene precursors. Figure 5a shows that the mass-specific radical yields of SOA decrease with

369   increasing relative concentrations of naphthalene (i.e., [naphthalene]/([naphthalene]+[β-pinene])). As the

370   relative concentration of naphthalene is increased from 0 to 9, 23, and 38%, the radical yields of SOA

371   decrease in the order of ~8.4 > ~3.0 > ~2.3 > ~1.9 pmol µg^{-1}. This is because the naphthalene SOA has a

372   lower radical yield than β-pinene SOA with the same mass concentration in water extracts (Tong et al.,

373   2016a;Tong et al., 2017;Tong et al., 2018;Tong et al., 2019). Moreover, the mass-specific radical yield of

374   β-pinene SOA in Figure 5a is the mean value of SOA from ~1 ppm and ~2.5 ppm of β-pinene (see Sect.

375   2.3). Therein the SOA from ~2.5 ppm β-pinene exhibits higher radical yield (11.5 pmol µg^{-1}) than the SOA

376   generated from ~1 ppm β-pinene (4.5 pmol µg^{-1}), which may be associated with the increasing partition of

377   oligomers into the particle phase with higher starting concentration of β-pinene (Kourtchev et al., 2016).

378   Some oligomers contain peroxide functional groups accounting for a major fraction of HOMs (Krapf et al.,

379   2016). The radical yield of naphthalene SOA in Figure 5 is the average yields of SOA formed by the

380   oxidation of ~0.2 ppm and ~0.6 ppm naphthalene (see section 2.3), respectively. Therein the radical yield

381   of SOA from ~0.2 ppm naphthalene (1.1 pmol μg^{-1}) is slightly higher than the SOA from ~0.6 ppm

382   naphthalene (0.8 pmol μg^{-1}), agreeing with the finding of enhanced oxidative potential of naphthalene SOA

383   formed under higher oxidant/naphthalene ratio condition (Wang et al., 2018b).

384   Figure 5b shows that β-pinene SOA mainly generates $^{\bullet}OH$ (~86%), whereas the mixed precursor SOA

385   and naphthalene SOA mainly generate $O_2^{\bullet-}$ (60-77%) and C-centered radicals (18-34%), which is in line

386   with our previous findings (Tong et al., 2016a;Tong et al., 2018;Tong et al., 2019). The much lower RF of

387    $^{\bullet}OH$ formed by mixed precursor SOA (< 10%) may mainly be due to its lower abundance of peroxide-

388   containing HOMs. It is notable that $PM_{2.5}$ from polluted Beijing contains substantial amount of aromatics

389   (Figure 4b), but mainly generates $^{\bullet}OH$ upon interaction with water, which seems to contradict our finding

390   that naphthalene SOA generates $^{\bullet}OH$ only to a small extent. This may be related to the more complex

391   composition of the ambient PM compared to laboratory-generated SOA. For example, conversion of $O_2^{\bullet-}$

392   to $^{\bullet}OH$, H_2O_2, and O_2 by transition metals or other redox-active PM constituents through Haber-Weiss

393   reactions or other related redox chemistry (Kehrer, 2000;Tong et al., 2016a) is expected to occur in ambient

394   samples, but would not be observed in laboratory-generated SOA that does not contain significant fractions

395   of transition metals.

396   **3.5 Radical yield of surrogate mixtures comprising transition metals, CHP, HA, FA and H₂O₂**

397   Figure 6a shows the concentration of radicals formed in aqueous mixtures comprising 0-25 μM cumene

398   hydroperoxide (CHP), 43 μM Fe^{2+}, 3 μM Cu^{2+}, 4 μg mL^{-1} humic acid (HA) and 7 μM H_2O_2, with mixtures

399   containing 0, 5, and 25 μM CHP to be treated as surrogates of redox-active constituents in PM from Beijing,

400   Mainz, and Hyytiälä. As the concentration of CHP is increased from 0 to 25 μM, the total concentration of

401   detectable radicals increases from 0.4 to 2.8 μM, with the relative fractions (RF) of C-centered radicals

402   increase from 1% to 30%, whereas the RF of $^{\bullet}OH$ and O-centered organic radicals decreases from 72% to

16

Atmospheric
Chemistry
and Physics
Discussions
Open Access
EGU

403   60% and from ~23% to ~8% (Figure 6b), respectively. The higher RF of C-centered radicals but lower RF

404   of $^\bullet$OH formed at higher concentration of CHP resembles the radical yield of ambient fine PM from cleaner

405   areas (Figure 2b), which contains a large fraction of HOMs (Tong et al., 2019). Moreover, Figure S5 shows

406   that adding 75, 100, 150, 200, and 300 μM H_2O_2 significantly and linearly (R^2=0.95) elevates the $^\bullet$OH

407   concentration in aqueous mixtures comprising CHP, Fe^{2+}, HA, and H_2O_2. Thus, the higher RF of $^\bullet$OH in

408   surrogate mixtures (Figure 6b) compared with ambient PM extracts (Figure 2b) may be due to the choice

409   of a slightly higher concentration of H_2O_2 in the surrogate mixture (7 μM, see SI).

410   To compare the Fenton-like reactions initiated by different transition metal ions related to ambient $PM_{2.5}$,

411   we measured the absolute and relative racial yields of aqueous mixtures containing CHP and different

412   transition metal species, such as Fe^{2+}, Cu^{2+}, Mn^{2+}, or Ni^{2+}. We found that Fe^{2+} is most efficient in initiating

413   Fenton-like reactions (Deguillaume et al., 2005) and the BMPO-radical adduct concentrations varied along

414   the reaction time (Figure S6). Of note, the abundance, chemical composition, and physicochemical

415   properties of the redox-active constituents in ambient PM (e.g., transition metals and organic matter) can

416   be different from the surrogate mixtures, causing partially different radical yields between surrogate

417   mixtures and ambient $PM_{2.5}$ (e.g., less comparable RF of $^\bullet$OH than the RF of C-centered radicals), which

418   warrants follow-up studies. To simplify the discussion, we only show the radical yields as mean values

419   within ~25 minutes of extraction and measurement.

420   To assess the influence of humic acid on Fenton-like reactions, we measured the radical yields of

421   mixtures comprising 100 μM CHP, 300 μM Fe^{2+}, and 0-180 μg mL^{-1} HA. As the concentration of HA is

422   increased from 0 to 36 μg mL^{-1}, the concentration of total formed radicals decreased by ~52% from 15.5 to

423   7.4 μM (Figure 6c). This may be associated with the following properties of HA. First, HA exhibits

424   pronounced iron binding capacity of 32 nmol Fe per milligram of HA, preferentially toward Fe^{3+} rather than

425   Fe^{2+} (Laglera and van den Berg, 2009;Scheinhardt et al., 2013). Thus, HA may interfere in the redox cycling

426   of Fe^{2+} and Fe^{3+} by chelating them. The lower concentration of free iron ions may prevent the formation

427   of radicals via Fenton-like reactions. Second, humic substances have been found to exhibit antioxidant

428   properties (Aeschbacher et al., 2012), thus the HA used for Figure 6c may act as an RS scavenger, therefore

429   terminating radical processes and reducing the overall radical concentration. As the HA concentration is

430   increased further from 36 to 180 µg mL^{-1}, the radical concentration is reduced slightly, by less than 20%.

431   This plateau of radical concentration is accompanied by an increasing RF of C-centered radicals (Figure

432   6d), indicating that HA may also be involved in more complex radical chemistry with $O_2^{\bullet-}$, $^{\bullet}OH$, or oxygen-

433   centered organic radicals enhancing carbon-centered radical formation (Shi et al., 2020). In fact, the RF of

434   C-centered radicals steeply increases from ~19% to ~94% as the HA concentration is increased from 0 to

435   180 µg mL^{-1}, whereas the RF of $O_2^{\bullet-}$ and $^{\bullet}OH$ decreases from ~59% and ~21% to ~3%. The higher RF of

436   C-centered radicals but lower RF of $O_2^{\bullet-}$ and $^{\bullet}OH$ at higher concentration of HA may be induced by the

437   reactions of HA with $O_2^{\bullet-}$ and $^{\bullet}OH$. The RF of O-centered organic radicals does not exhibit a consistent

438   trend and varies within the range of 5-20%. Moreover, we found that the reaction between HA and CHP

439   (in the absence of Fe ions) produces only a negligible amount of radicals (not shown), which indicates that

440   HA may mainly influence the radical formation upon interaction with iron ions or radicals formed by

441   Fenton-like reactions, but does not form prominent amount of radicals by reactions with CHP or through

442   the decomposition of CHP at the applied concentrations.

443   Fulvic acid (FA) is another kind of typical atmospheric humic-like substances exerting metal chelating

444   activity (Graber and Rudich, 2006; Tang et al., 2014). Thus, we also measured the radical yields of the

445   mixtures comprising CHP, transition metals, and FA. As shown in Figure 6e, the concentration of radicals

446   formed by mixtures comprising 100 µM CHP, 300 µM Fe^{2+}, and FA decreases by ~10% as the

447   concentration of FA is increased from 6 to 36 µg mL^{-1}. Therein the $O_2^{\bullet-}$ is the dominant radial species,

448   accounting for > 59% of totally formed radicals (Figure 6f). The $O_2^{\bullet-}$ may be generated via multiple redox

449   reaction pathways such as oxidation of Fe^{2+} or decomposition of organic peroxy radicals (Chevallier et al.,

450   2004). Figure 6f also shows that RF of $^{\bullet}OH$, $O_2^{\bullet-}$, C- and O-centered organic radicals varies slightly, which

451   is different from the decreasing radical yield by Fenton-like reaction system containing HA (Figure 6c), but

452   agreeing with the lower capacity of FA (16.7±2.0 nmol mg^{-1}) than HA (32.0±2.2 nmol mg^{-1}) in binding

453   Fe(III) (Laglera and van den Berg, 2009). As the concentration of FA is increased further to 12 µg mL^{-1},

454   the observed radical concentration in aqueous mixtures of CHP+Fe^{2+}+FA decreases significantly to ~9.6

455   µM, which may mainly be associated with the formation of Fe-FA complexes and the radical scavenging

456   effect of FA as discussed for HA above (Wang et al., 1996;Scheinhardt et al., 2013;Yang et al., 2017).

457   During this process, the RF of C-centered radicals increases for 3-fold to be ~28%, indicating that FA may

458   also be oxidized by different types of oxidants to form C-centered radicals (Gonzalez et al., 2017), similar

459   to HA in Figure 6c. As the concentration of FA is increased further to 180 µg mL^{-1}, the concentration of

460   totally formed radicals decreases further to 7.6 µM, the RF of C-centered radicals increases further to ~36%,

461   whereas the RF of $\cdot$OH and O-centered organic radicals decreases significantly to 4-5% and below the

462   detecting limit, respectively (Figure 6f). Moreover, the Figure S7 indicates that the RF of different radicals

463   formed by mixtures comprising CHP, Cu^{2+} and FA exhibited a different trend from the mixtures of CHP,

464   Fe^{2+}, and FA, indicating that FA might influence the radical formation by Cu^{2+} initiated Fenton-like

465   reactions in a efficiency different from the Fe^{2+} initiated Fenton-like reactions.

466   **4 Conclusions and implications**

467   In this study, we found that PM$_{2.5}$ levels exhibit a negative correlation with the mass-specific radical yields,

468   but a weak positive correlation with the H$_2$O$_2$ yields. We also found that the mass-specific concentration of

469   transition metals and relative abundance of aromatic compounds are higher in the urban air than the remote

470   forest, in the order of Hyytiälä < Mainz < Beijing. The relative fractions (RF) of $\cdot$OH formed by different

471   source PM$_{2.5}$ in water is in the same order as the relative abundances of transition metals and aromatics,

472   indicating that urban fine PM favors the formation of OH radicals upon redox chemistry of transition metals,

473   aromatics, or transition metal-aromatic interactions in water. The relative abundance of highly oxygenated

474   organic molecules (HOMs) exhibits a reverse trend compared to aromatics and transition metals, but is in

475   a positive correlation with the RF of C-centered radicals, confirming the strong association of HOMs with

476   organic radical formation by PM$_{2.5}$ in water (Tong et al., 2019).

477   We also measured the radical yield of laboratory-generated SOA from mixing the biogenic SOA

478   precursor β-pinene and the anthropogenic SOA precursor naphthalene. We found that the relative fractions

479   of naphthalene SOA of the totally formed SOA significantly influence the amount and types of radicals

480   formed by the mixed precursor SOA in water with $^{\bullet}$OH radicals dominating pure β-pinene SOA, Carbon-

481   centered radicals becoming increasingly dominant as the fraction of naphthalene increases. To get insights

482   into the Fenton-like reactions in aqueous extracts of ambient $PM_{2.5}$, we investigated the radical formation

483   by surrogate mixtures comprising cumene hydroperoxide, transition metals, water-soluble humic acid (HA)

484   or fulvic acid (FA), and H_2O_2. We found that HA and FA exhibit different radical scavenging and

485   antioxidant activity in suppressing the radical formation from Fenton-like reactions.

486   The synthetic application of ambient $PM_{2.5}$ characterization, chamber simulation, and surrogate mixture

487   measurement in this study provides a novel approach to investigate the RS chemistry of atmospheric

488   particles. The direct analysis of ambient $PM_{2.5}$ enables us to find and quantify the key component (e.g.,

489   HOMs, aromatics, or transition metals) of $PM_{2.5}$ that may influence its reactivity. The investigation of

490   laboratory-generated SOA enables us to assess the influence of anthropogenic-biogenic organic component

491   interactions on the radical formation by ambient PM. The measurement of surrogate or aqueous mixtures

492   of model substances (transition metals, CHP, HA, FA, and H_2O_2) enables us to clarify the role of individual

493   redox active compound as well as their interplays in the radical chemistry of PM, including Fenton-like

494   reactions, transition metal-organic interactions, or subsequent chain reactions. Based on this systematic

495   analysis, we quantitatively compared the RS formation mechanism of particulate matter from air ranging

496   from clean to heavily polluted areas. The higher relative amount of detected radicals and H_2O_2 formed by

497   urban $PM_{2.5}$ can be seen as a measure of higher potential oxidative damage caused by air pollutants in the

498   epithelial lining fluid of the human respiratory tract. These newly achieved insights enable a better

499   understanding of the influence of biogenic and anthropogenic emissions on atmospheric chemistry, air

500   quality, and public health in the Anthropocene (Pöschl and Shiraiwa, 2015;Cheng et al., 2016;Shiraiwa et

501   al., 2017). Finally, the composition and concentration of organic molecules have been found to influence

502   its role in transition metal-initiated radical chemistry. For instance, carboxylic acids enhance the oxidative

Atmospheric
Chemistry
and Physics
Discussions

503   potential of transition metals, whereas the imidazoles suppress it (Lin and Yu, 2020). Moreover, low

504   concentration of oxalate forms mono-complexes with Fe^{2+}, but high concentration of oxalate scavenges OH

505   radicals (Fang et al., 2020). Thus, the role of different humic-like substances component in Fenton-like

506   reactions and its impact on aerosol reactivity have not been fully addressed, which warrants follow up

507   studies.

508 **References**

509 Aeschbacher, M., Graf, C., Schwarzenbach, R. P., and Sander, M.: Antioxidant properties of humic
510 substances, Environ. Sci. Technol., 46, 4916-4925, 2012.

511 An, Z., Huang, R.-J., Zhang, R., Tie, X., Li, G., Cao, J., Zhou, W., Shi, Z., Han, Y., and Gu, Z.: Severe
512 haze in Northern China: A synergy of anthropogenic emissions and atmospheric processes, Proc. Natl. Acad.
513 Sci. U.S.A., 116, 8657-8666, 2019.

514 Anglada, J. M., Martins-Costa, M., Francisco, J. S., and Ruiz-Lopez, M. F.: Interconnection of reactive
515 oxygen species chemistry across the interfaces of atmospheric, environmental, and biological processes,
516 Acc. Chem. Res., 48, 575-583, 2015.

517 Arangio, A. M., Tong, H., Socorro, J., Pöschl, U., and Shiraiwa, M.: Quantification of environmentally
518 persistent free radicals and reactive oxygen species in atmospheric aerosol particles, Atmos. Chem. Phys.,
519 16, 13105-13119, 2016.

520 Arellanes, C., Paulson, S. E., Fine, P. M., and Sioutas, C.: Exceeding of Henry's law by hydrogen peroxide
521 associated with urban aerosols, Environ. Sci. Technol., 40, 4859-4866, 2006.

522 Badali, K., Zhou, S., Aljawhary, D., Antiñolo, M., Chen, W., Lok, A., Mungall, E., Wong, J., Zhao, R., and
523 Abbatt, J.: Formation of hydroxyl radicals from photolysis of secondary organic aerosol material, Atmos.
524 Chem. Phys., 15, 7831-7840, 2015.

525 Bates, J. T., Weber, R. J., Abrams, J., Verma, V., Fang, T., Klein, M., Strickland, M. J., Sarnat, S. E., Chang,
526 H. H., and Mulholland, J. A.: Reactive oxygen species generation linked to sources of atmospheric
527 particulate matter and cardiorespiratory effects, Environ. Sci. Technol., 49, 13605-13612, 2015.

528 Bates, J. T., Fang, T., Verma, V., Zeng, L., Weber, R. J., Tolbert, P. E., Abrams, J. Y., Sarnat, S. E., Klein,
529 M., Mulholland, J. A., and Russell, A. G.: Review of acellular assays of ambient particulate matter oxidative
530 potential: Methods and relationships with composition, sources, and health effects, Environ. Sci. Technol.,
531 53, 4003-4019, 2019.

532 Baumgartner, J., Zhang, Y., Schauer, J. J., Huang, W., Wang, Y., and Ezzati, M.: Highway proximity and
533 black carbon from cookstoves as a risk factor for higher blood pressure in rural China, Proc. Natl. Acad.
534 Sci. U.S.A., 111, 13229-13234, 2014.

535 Catrouillet, C., Davranche, M., Dia, A., Bouhnik-Le Coz, M., Marsac, R., Pourret, O., and Gruau, G.:
536 Geochemical modeling of Fe (II) binding to humic and fulvic acids, Chem. Geol., 372, 109-118, 2014.

537 Charrier, J., and Anastasio, C.: On dithiothreitol (DTT) as a measure of oxidative potential for ambient
538 particles: evidence for the importance of soluble transition metals, Atmos. Chem. Phys., 12, 9321-9333,
539 2012.

540   Charrier, J. G., McFall, A. S., Richards-Henderson, N. K., and Anastasio, C.: Hydrogen peroxide formation
541   in a surrogate lung fluid by transition metals and quinones present in particulate matter, Environ. Sci.
542   Technol., 48, 7010-7017, 2014.

543   Charrier, J. G., and Anastasio, C.: Rates of hydroxyl radical production from transition metals and quinones
544   in a surrogate lung fluid, Environ. Sci. Technol., 49, 9317-9325, 2015.

545   Chen, X., Hopke, P. K., and Carter, W. P.: Secondary organic aerosol from ozonolysis of biogenic volatile
546   organic compounds: chamber studies of particle and reactive oxygen species formation, Environ. Sci.
547   Technol., 45, 276-282, 2010.

548   Cheng, C., Li, M., Chan, C. K., Tong, H., Chen, C., Chen, D., Wu, D., Li, L., Wu, C., and Cheng, P.: Mixing
549   state of oxalic acid containing particles in the rural area of Pearl River Delta, China: implications for the
550   formation mechanism of oxalic acid, Atmos. Chem. Phys., 17, 9519-9533, 2017.

551   Cheng, Y., Zheng, G., Wei, C., Mu, Q., Zheng, B., Wang, Z., Gao, M., Zhang, Q., He, K., and Carmichael,
552   G.: Reactive nitrogen chemistry in aerosol water as a source of sulfate during haze events in China, Sci.
553   Adv., 2, e1601530, 2016.

554   Chevallier, E., Jolibois, R. D., Meunier, N., Carlier, P., and Monod, A.: "Fenton-like" reactions of
555   methylhydroperoxide and ethylhydroperoxide with Fe^{2+} in liquid aerosols under tropospheric conditions,
556   Atmos. Environ., 38, 921-933, 2004.

557   Chowdhury, P. H., He, Q., Carmieli, R., Li, C., Rudich, Y., and Pardo, M.: Connecting the Oxidative
558   Potential of Secondary Organic Aerosols with Reactive Oxygen Species in Exposed Lung Cells, Environ.
559   Sci. Technol., 53, 13949-13958, 2019.

560   Chung, M. Y., Lazaro, R. A., Lim, D., Jackson, J., Lyon, J., Rendulic, D., and Hasson, A. S.: Aerosol-borne
561   quinones and reactive oxygen species generation by particulate matter extracts, Environ. Sci. Technol., 40,
562   4880-4886, 2006.

563   Crobeddu, B., Baudrimont, I., Deweirdt, J., Sciare, J., Badel, A., Camproux, A.-C., Bui, L. C., and Baeza-
564   Squiban, A.: Lung Antioxidant Depletion: A Predictive Indicator of Cellular Stress Induced by Ambient
565   Fine Particles, Environ. Sci. Technol., 54, 2360-2369, 2020.

566   Cui, Y., Xie, X., Jia, F., He, J., Li, Z., Fu, M., Hao, H., Liu, Y., Liu, J. Z., and Cowan, P. J.: Ambient fine
567   particulate matter induces apoptosis of endothelial progenitor cells through reactive oxygen species
568   formation, Cell Physiol. Biochem., 35, 353-363, 2015.

569   De Araujo, M., De M. Carneiro, J., and Taranto, A.: Solvent effects on the relative stability of radicals
570   derived from artemisinin: DFT study using the PCM/COSMO approach, Int. J. Quantum. Chem., 106,
571   2804-2810, 2006.

572   Deguillaume, L., Leriche, M., Desboeufs, K., Mailhot, G., George, C., and Chaumerliac, N.: Transition
573   metals in atmospheric liquid phases: Sources, reactivity, and sensitive parameters, Chem. Rev., 105, 3388-
574   3431, 2005.

575   Donaldson, D., and Valsaraj, K. T.: Adsorption and reaction of trace gas-phase organic compounds on
576   atmospheric water film surfaces: A critical review, Environ. Sci. Technol., 44, 865-873, 2010.

577   Ehn, M., Thornton, J. A., Kleist, E., Sipilä, M., Junninen, H., Pullinen, I., Springer, M., Rubach, F.,
578   Tillmann, R., and Lee, B.: A large source of low-volatility secondary organic aerosol, Nature, 506, 476-
579   479, 2014.

580   Elser, M., Huang, R.-J., Wolf, R., Slowik, J. G., Wang, Q., Canonaco, F., Li, G., Bozzetti, C., Daellenbach,
581   K. R., and Huang, Y.: New insights into $PM_{2.5}$ chemical composition and sources in two major cities in
582   China during extreme haze events using aerosol mass spectrometry, Atmos. Chem. Phys., 16, 3207-3225,
583   2016.

584   Enami, S., Sakamoto, Y., and Colussi, A. J.: Fenton chemistry at aqueous interfaces, Proc. Natl. Acad. Sci.
585   U.S.A., 111, 623-628, 2014.

586   Ervens, B., Turpin, B., and Weber, R.: Secondary organic aerosol formation in cloud droplets and aqueous
587   particles (aqSOA): a review of laboratory, field and model studies, Atmos. Chem. Phys., 11, 11069-11102,
588   2011.

589   Fan, X., Wei, S., Zhu, M., Song, J., and Peng, P. a.: Comprehensive characterization of humic-like
590   substances in smoke $PM_{2.5}$ emitted from the combustion of biomass materials and fossil fuels, Atmos. Chem.
591   Phys., 16, 13321-13340, 2016.

592   Fang, T., Guo, H., Verma, V., Peltier, R., and Weber, R.: $PM_{2.5}$ water-soluble elements in the southeastern
593   United States: automated analytical method development, spatiotemporal distributions, source
594   apportionment, and implications for heath studies, Atmos. Chem. Phys., 15, 11667-11682, 2015.

595   Fang, T., Verma, V., Bates, J. T., Abrams, J., Klein, M., Strickland, M. J., Sarnat, S. E., Chang, H. H.,
596   Mulholland, J. A., and Tolbert, P. E.: Oxidative potential of ambient water-soluble $PM_{2.5}$ in the southeastern
597   United States: contrasts in sources and health associations between ascorbic acid (AA) and dithiothreitol
598   (DTT) assays, Atmos. Chem. Phys., 16, 3865-3879, 2016.

599   Fang, T., Lakey, P. S. J., Weber, R. J., and Shiraiwa, M.: Oxidative Potential of Particulate Matter and
600   Generation of Reactive Oxygen Species in Epithelial Lining Fluid, Environ. Sci. Technol., 53, 12784-12792,
601   2019.

602   Fang, T., Lakey, P. S. J., Rivera-Rios, J. C., Keutsch, F. N., and Shiraiwa, M.: Aqueous-Phase
603   Decomposition of Isoprene Hydroxy Hydroperoxide and Hydroxyl Radical Formation by Fenton-Like
604   Reactions with Iron Ions, J. Phys. Chem. A, 124, 5230-5236, 2020.

Gehling, W., Khachatryan, L., and Dellinger, B.: Hydroxyl radical generation from environmentally persistent free radicals (EPFRs) in PM$_{2.5}$, Environ. Sci. Technol., 48, 4266-4272, 2014.

Gilardoni, S., Massoli, P., Paglione, M., Giulianelli, L., Carbone, C., Rinaldi, M., Decesari, S., Sandrini, S., Costabile, F., and Gobbi, G. P.: Direct observation of aqueous secondary organic aerosol from biomass-burning emissions, Proc. Natl. Acad. Sci. U.S.A., 113, 10013-10018, 2016.

Gligorovski, S., Strekowski, R., Barbati, S., and Vione, D.: Environmental implications of hydroxyl radicals (·OH), Chem. Rev., 115, 13051-13092, 2015.

Goldstein, A. H., Koven, C. D., Heald, C. L., and Fung, I. Y.: Biogenic carbon and anthropogenic pollutants combine to form a cooling haze over the southeastern United States, Proc. Natl. Acad. Sci. U.S.A., 106, 8835-8840, 2009.

Gonzalez, D. H., Cala, C. K., Peng, Q., and Paulson, S. E.: HULIS enhancement of hydroxyl radical formation from Fe(II): Kinetics of fulvic acid–Fe(II) complexes in the presence of lung antioxidants, Environ. Sci. Technol., 51, 7676-7685, 2017.

Graber, E., and Rudich, Y.: Atmospheric HULIS: How humic-like are they? A comprehensive and critical review, Atmos. Chem. Phys., 6, 729-753, 2006.

Hakola, H., Hellén, H., Hemmilä, M., Rinne, J., and Kulmala, M.: In situ measurements of volatile organic compounds in a boreal forest, Atmos. Chem. Phys., 12, 11665-11678, 2012.

Halliwell, B., and Whiteman, M.: Measuring reactive species and oxidative damage in vivo and in cell culture: how should you do it and what do the results mean?, Br. J. Pharmacol., 142, 231-255, 2004.

Hari, P., and Kulmala, M.: Station for Measuring EcosystemsAtmosphere Relations (SMEAR II), Boreal Env. Res., 10, 315-322, 2005.

Hoyle, C. R., Boy, M., Donahue, N. M., Fry, J. L., Glasius, M., Guenther, A., Hallar, A. G., Huff Hartz, K., Petters, M. D., and Petäjä, T.: A review of the anthropogenic influence on biogenic secondary organic aerosol, Atmos. Chem. Phys., 11, 321-343, 2011.

Huang, G., Liu, Y., Shao, M., Li, Y., Chen, Q., Zheng, Y., Wu, Z., Liu, Y., Wu, Y., Hu, M., Li, X., Lu, S., Wang, C., Liu, J., Zheng, M., and Zhu, T.: Potentially Important Contribution of Gas-Phase Oxidation of Naphthalene and Methylnaphthalene to Secondary Organic Aerosol during Haze Events in Beijing, Environ. Sci. Technol., 53, 1235-1244, 2019.

Huang, R.-J., Zhang, Y., Bozzetti, C., Ho, K.-F., Cao, J.-J., Han, Y., Daellenbach, K. R., Slowik, J. G., Platt, S. M., and Canonaco, F.: High secondary aerosol contribution to particulate pollution during haze events in China, Nature, 514, 218-222, 2014.

Jacob, D. J.: Heterogeneous chemistry and tropospheric ozone, Atmos. Environ., 34, 2131-2159, 2000.

Jimenez, J. L., Canagaratna, M., Donahue, N., Prevot, A., Zhang, Q., Kroll, J. H., DeCarlo, P. F., Allan, J. D., Coe, H., and Ng, N.: Evolution of organic aerosols in the atmosphere, Science, 326, 1525-1529, 2009.

639   Jin, L., Xie, J., Wong, C. K., Chan, S. K., Abbaszade, G. l., Schnelle-Kreis, J. r., Zimmermann, R., Li, J.,

640   Zhang, G., and Fu, P.: Contributions of city-specific fine particulate matter ($PM_{2.5}$) to differential in vitro

641   oxidative stress and toxicity implications between Beijing and Guangzhou of China, Environ. Sci. Technol.,

642   53, 2881-2891, 2019.

643   Kalyanaraman, B., Darley-Usmar, V., Davies, K. J., Dennery, P. A., Forman, H. J., Grisham, M. B., Mann,

644   G. E., Moore, K., Roberts II, L. J., and Ischiropoulos, H.: Measuring reactive oxygen and nitrogen species

645   with fluorescent probes: challenges and limitations, Free Radic. Biol. Med., 52, 1-6, 2012.

646   Kang, E., Root, M., Toohey, D., and Brune, W. H.: Introducing the concept of potential aerosol mass (PAM),

647   Atmos. Chem. Phys., 7, 5727-5744, 2007.

648   Kehrer, J. P.: The Haber–Weiss reaction and mechanisms of toxicity, Toxicology, 149, 43-50, 2000.

649   Khachatryan, L., Vejerano, E., Lomnicki, S., and Dellinger, B.: Environmentally persistent free radicals

650   (EPFRs). 1. Generation of reactive oxygen species in aqueous solutions, Environ. Sci. Technol., 45, 8559-

651   8566, 2011.

652   Koch, B., and Dittmar, T.: From mass to structure: An aromaticity index for high‐resolution mass data of

653   natural organic matter, Rapid Commun. Mass Spectrom., 20, 926-932, 2006.

654   Kostić, I., Anđelković, T., Nikolić, R., Bojić, A., Purenović, M., Blagojević, S., and Anđelković, D.:

655   Copper(II) and lead(II) complexation by humic acid and humic-like ligands, J. Serb. Chem. Soc., 76, 1325-

656   1336, 2011.

657   Kourtchev, I., Giorio, C., Manninen, A., Wilson, E., Mahon, B., Aalto, J., Kajos, M., Venables, D.,

658   Ruuskanen, T., and Levula, J.: Enhanced volatile organic compounds emissions and organic aerosol mass

659   increase the oligomer content of atmospheric aerosols, Sci. Rep., 6, 35038, 2016.

660   Krapf, M., El Haddad, I., Bruns, E. A., Molteni, U., Daellenbach, K. R., Prévôt, A. S., Baltensperger, U.,

661   and Dommen, J.: Labile peroxides in secondary organic aerosol, Chem, 1, 603-616, 2016.

662   Kuang, X. M., Scott, J. A., da Rocha, G. O., Betha, R., Price, D. J., Russell, L. M., Cocker, D. R., and

663   Paulson, S. E.: Hydroxyl radical formation and soluble trace metal content in particulate matter from

664   renewable diesel and ultra low sulfur diesel in at-sea operations of a research vessel, Aerosol Sci. Technol.,

665   51, 147-158, 2017.

666   Laakso, L., Hussein, T., Aarnio, P., Komppula, M., Hiltunen, V., Viisanen, Y., and Kulmala, M.: Diurnal

667   and annual characteristics of particle mass and number concentrations in urban, rural and Arctic

668   environments in Finland, Atmos. Environ., 37, 2629-2641, 2003.

669   Laglera, L. M., and van den Berg, C. M.: Evidence for geochemical control of iron by humic substances in

670   seawater, Limnol. Oceanogr., 54, 610-619, 2009.

671   Lakey, P. S., Berkemeier, T., Tong, H., Arangio, A. M., Lucas, K., Pöschl, U., and Shiraiwa, M.: Chemical
672   exposure-response relationship between air pollutants and reactive oxygen species in the human respiratory
673   tract, Sci. Rep., 6, 32916, 2016.

674   Landreman, A. P., Shafer, M. M., Hemming, J. C., Hannigan, M. P., and Schauer, J. J.: A macrophage-
675   based method for the assessment of the reactive oxygen species (ROS) activity of atmospheric particulate
676   matter (PM) and application to routine (daily-24 h) aerosol monitoring studies, Aerosol Sci. Technol., 42,
677   946-957, 2008.

678   Lelieveld, J., and Pöschl, U.: Chemists can help to solve the air-pollution health crisis, Nature, 551, 291-
679   293, 2017.

680   Li, N., Xia, T., and Nel, A. E.: The role of oxidative stress in ambient particulate matter-induced lung
681   diseases and its implications in the toxicity of engineered nanoparticles, Free Radic. Biol. Med., 44, 1689-
682   1699, 2008.

683   Li, X., Kuang, X. M., Yan, C., Ma, S., Paulson, S. E., Zhu, T., Zhang, Y., and Zheng, M.: Oxidative
684   potential by $PM_{2.5}$ in the North China Plain: generation of hydroxyl radical, Environ. Sci. Technol., 53,
685   512-520, 2018.

686   Lin, M., and Yu, J. Z.: Assessment of interactions between transition metals and atmospheric organics:
687   Ascorbic Acid Depletion and Hydroxyl Radical Formation in Organic-metal Mixtures, Environ. Sci.
688   Technol., 54, 1431−1442, 2020.

689   Lin, P., and Yu, J. Z.: Generation of reactive oxygen species mediated by humic-like substances in
690   atmospheric aerosols, Environ. Sci. Technol., 45, 10362-10368, 2011.

691   Lin, Y., Ma, Y., Qiu, X., Li, R., Fang, Y., Wang, J., Zhu, Y., and Hu, D.: Sources, transformation, and
692   health implications of PAHs and their nitrated, hydroxylated, and oxygenated derivatives in $PM_{2.5}$ in Beijing,
693   J. Geophys. Res. Atmos., 120, 7219-7228, 2015.

694   Liu, F., Saavedra, M. G., Champion, J. A., Griendling, K. K., and Ng, N. L.: Prominent Contribution of
695   Hydrogen Peroxide to Intracellular Reactive Oxygen Species Generated upon Exposure to Naphthalene
696   Secondary Organic Aerosols, Environ. Sci. Technol. Lett., 7, 171-177, 2020.

697   Liu, Q., Baumgartner, J., Zhang, Y., Liu, Y., Sun, Y., and Zhang, M.: Oxidative potential and inflammatory
698   impacts of source apportioned ambient air pollution in Beijing, Environ. Sci. Technol., 48, 12920-12929,
699   2014.

700   Ma, Y., Cheng, Y., Qiu, X., Cao, G., Fang, Y., Wang, J., Zhu, T., Yu, J., and Hu, D.: Sources and oxidative
701   potential of water-soluble humic-like substances (HULIS WS) in fine particulate matter ($PM_{2.5}$) in Beijing,
702   Atmos. Chem. Phys., 18, 5607-5617, 2018.

703   Maenhaut, W., Nava, S., Lucarelli, F., Wang, W., Chi, X., and Kulmala, M.: Chemical composition, impact
704   from biomass burning, and mass closure for $PM_{2.5}$ and PM_{10} aerosols at Hyytiälä, Finland, in summer 2007,
705   X-Ray Spectrom., 40, 168-171, 2011.

706   Molina, C., Toro, R., Manzano, C., Canepari, S., Massimi, L., and Leiva-Guzmán, M. A.: Airborne aerosols
707   and human health: Leapfrogging from mass concentration to oxidative potential, Atmosphere, 11, 917,
708   2020.

709   Møller, P., Jacobsen, N. R., Folkmann, J. K., Danielsen, P. H., Mikkelsen, L., Hemmingsen, J. G., Vesterdal,
710   L. K., Forchhammer, L., Wallin, H., and Loft, S.: Role of oxidative damage in toxicity of particulates, Free
711   Radic. Res., 44, 1-46, 2010.

712   Nel, A.: Air pollution-related illness: effects of particles, Science, 308, 804-806, 2005.

713   Ohyama, M., Otake, T., Adachi, S., Kobayashi, T., and Morinaga, K.: A comparison of the production of
714   reactive oxygen species by suspended particulate matter and diesel exhaust particles with macrophages,
715   Inhal. Toxicol., 19, 157-160, 2007.

716   Page, S. E., Sander, M., Arnold, W. A., and McNeill, K.: Hydroxyl radical formation upon oxidation of
717   reduced humic acids by oxygen in the dark, Environ. Sci. Technol., 46, 1590-1597, 2012.

718   Park, J., Park, E. H., Schauer, J. J., Yi, S.-M., and Heo, J.: Reactive oxygen species (ROS) activity of
719   ambient fine particles ($PM_{2.5}$) measured in Seoul, Korea, Environ. Int., 117, 276-283, 2018.

720   Pöschl, U., and Shiraiwa, M.: Multiphase chemistry at the atmosphere–biosphere interface influencing
721   climate and public health in the anthropocene, Chem. Rev., 115, 4440-4475, 2015.

722   Pye, H. O., D'Ambro, E. L., Lee, B. H., Schobesberger, S., Takeuchi, M., Zhao, Y., Lopez-Hilfiker, F., Liu,
723   J., Shilling, J. E., and Xing, J.: Anthropogenic enhancements to production of highly oxygenated molecules
724   from autoxidation, Proc. Natl. Acad. Sci. U.S.A., 116, 6641-6646, 2019.

725   Qiu, J., Liang, Z., Tonokura, K., Colussi, A. J., and Enami, S.: Stability of Monoterpene-Derived α-
726   Hydroxyalkyl-Hydroperoxides in Aqueous Organic Media: Relevance to the Fate of Hydroperoxides in
727   Aerosol Particle Phases, Environ. Sci. Technol., 54, 3890-3899, 2020.

728   Qu, J., Li, Y., Zhong, W., Gao, P., and Hu, C.: Recent developments in the role of reactive oxygen species
729   in allergic asthma, J. Thorac. Dis., 9, E32, 2017.

730   Rao, X., Zhong, J., Brook, R. D., and Rajagopalan, S.: Effect of particulate matter air pollution on
731   cardiovascular oxidative stress pathways, Antioxid. Redox. Signal., 28, 797-818, 2018.

732   Reinmuth-Selzle, K., Kampf, C. J., Lucas, K., Lang-Yona, N., Fröhlich-Nowoisky, J., Shiraiwa, M., Lakey,
733   P. S., Lai, S., Liu, F., and Kunert, A. T.: Air pollution and climate change effects on allergies in the
734   anthropocene: abundance, interaction, and modification of allergens and adjuvants, Environ. Sci. Technol.,
735   51, 4119-4141, 2017.

736 Scheinhardt, S., Müller, K., Spindler, G., and Herrmann, H.: Complexation of trace metals in size-

737 segregated aerosol particles at nine sites in Germany, Atmos. Environ., 74, 102-109, 2013.

738 Shi, Y., Dai, Y., Liu, Z., Nie, X., Zhao, S., Zhang, C., and Jia, H.: Light-induced variation in

739 environmentally persistent free radicals and the generation of reactive radical species in humic substances,

740 Front. Environ. Sci. Eng., 14, 1-10, 2020.

741 Shiraiwa, M., Ueda, K., Pozzer, A., Lammel, G., Kampf, C. J., Fushimi, A., Enami, S., Arangio, A. M.,

742 Fröhlich-Nowoisky, J., Fujitani, Y., Furuyama, A., Lakey, P. S. J., Lelieveld, J., Lucas, K., Morino, Y.,

743 Pöschl, U., Takahama, S., Takami, A., Tong, H., Weber, B., Yoshino, A., and Sato, K.: Aerosol health

744 effects from molecular to global scales, Environ. Sci. Technol., 51, 13545-13567, 2017.

745 Shrivastava, M., Andreae, M. O., Artaxo, P., Barbosa, H. M., Berg, L. K., Brito, J., Ching, J., Easter, R. C.,

746 Fan, J., and Fast, J. D.: Urban pollution greatly enhances formation of natural aerosols over the Amazon

747 rainforest, Nat. Commun., 10, 1046, 2019.

748 Sies, H., Berndt, C., and Jones, D. P.: Oxidative stress, Annu. Rev. Biochem., 86, 715-748, 2017.

749 Singh, D. K., and Gupta, T.: Role of transition metals with water soluble organic carbon in the formation

750 of secondary organic aerosol and metallo‐organics in PM_1 sampled during post monsoon and pre-winter

751 time, J. Aerosol Sci., 94, 56-69, 2016.

752 Tang, W.-W., Zeng, G.-M., Gong, J.-L., Liang, J., Xu, P., Zhang, C., and Huang, B.-B.: Impact of

753 humic/fulvic acid on the removal of heavy metals from aqueous solutions using nanomaterials: a review,

754 Sci. Total Environ., 468, 1014-1027, 2014.

755 Tong, H., Arangio, A. M., Lakey, P. S., Berkemeier, T., Liu, F., Kampf, C. J., Brune, W. H., Pöschl, U.,

756 and Shiraiwa, M.: Hydroxyl radicals from secondary organic aerosol decomposition in water, Atmos. Chem.

757 Phys., 16, 1761-1771, 2016a.

758 Tong, H., Kourtchev, I., Pant, P., Keyte, I. J., O'Connor, I. P., Wenger, J. C., Pope, F. D., Harrison, R. M.,

759 and Kalberer, M.: Molecular composition of organic aerosols at urban background and road tunnel sites

760 using ultra-high resolution mass spectrometry, Faraday Discuss., 189, 51-68, 2016b.

761 Tong, H., Lakey, P. S., Arangio, A. M., Socorro, J., Kampf, C. J., Berkemeier, T., Brune, W. H., Pöschl,

762 U., and Shiraiwa, M.: Reactive oxygen species formed in aqueous mixtures of secondary organic aerosols

763 and mineral dust influencing cloud chemistry and public health in the Anthropocene, Faraday Discuss., 200,

764 251-270, 2017.

765 Tong, H., Lakey, P. S., Arangio, A. M., Socorro, J., Shen, F., Lucas, K., Brune, W. H., Pöschl, U., and

766 Shiraiwa, M.: Reactive oxygen species formed by secondary organic aerosols in water and surrogate lung

767 fluid, Environ. Sci. Technol., 52, 11642-11651, 2018.

768 Tong, H., Zhang, Y., Filippi, A., Wang, T., Li, C., Liu, F., Leppla, D., Kourtchev, I., Wang, K., Keskinen,

769 H.-M., Levula, J. T., Arangio, A. M., Shen, F., Ditas, F., Martin, S. T., Artaxo, P., Godoi, R. H. M.,

770 Yamamoto, C. I., Souza, R. A. F. d., Huang, R.-J., Berkemeier, T., Wang, Y., Su, H., Cheng, Y., Pope, F.

771 D., Fu, P., Yao, M., Pöhlker, C., Petäjä, T., Kulmala, M., Andreae, M. O., Shiraiwa, M., Pöschl, U.,

772 Hoffmann, T., and Kalberer, M.: Radical Formation by Fine Particulate Matter Associated with Highly

773 Oxygenated Molecules, Environ. Sci. Technol., 53, 12506-12518, 2019.

774 Tröstl, J., Chuang, W. K., Gordon, H., Heinritzi, M., Yan, C., Molteni, U., Ahlm, L., Frege, C., Bianchi, F.,

775 and Wagner, R.: The role of low-volatility organic compounds in initial particle growth in the atmosphere,

776 Nature, 533, 527-531, 2016.

777 Tseitlin, M., Eaton, S. S., and Eaton, G. R.: Uncertainty analysis for absorption and first‐derivative

778 electron paramagnetic resonance spectra, Concepts Magn. Reson., Part A, 40, 295-305, 2012.

779 Valavanidis, A., Fiotakis, K., Bakeas, E., and Vlahogianni, T.: Electron paramagnetic resonance study of

780 the generation of reactive oxygen species catalysed by transition metals and quinoid redox cycling by

781 inhalable ambient particulate matter, Redox. Rep., 10, 37-51, 2005.

782 Verma, V., Fang, T., Guo, H., King, L., Bates, J., Peltier, R., Edgerton, E., Russell, A., and Weber, R.:

783 Reactive oxygen species associated with water-soluble $PM_{2.5}$ in the southeastern United States:

784 spatiotemporal trends and source apportionment, Atmos. Chem. Phys., 14, 12915-12930, 2014.

785 Verma, V., Fang, T., Xu, L., Peltier, R. E., Russell, A. G., Ng, N. L., and Weber, R. J.: Organic aerosols

786 associated with the generation of reactive oxygen species (ROS) by water-soluble $PM_{2.5}$, Environ. Sci.

787 Technol., 49, 4646-4656, 2015.

788 Wang, C., Wang, Z., Peng, A., Hou, J., and Xin, W.: Interaction between fulvic acids of different origins

789 and active oxygen radicals, Sci. China C Life Sci., 39, 267-275, 1996.

790 Wang, K., Zhang, Y., Huang, R.-J., Cao, J., and Hoffmann, T.: UHPLC-Orbitrap mass spectrometric

791 characterization of organic aerosol from a central European city (Mainz, Germany) and a Chinese megacity

792 (Beijing), Atmos. Environ., 189, 22-29, 2018a.

793 Wang, K., Zhang, Y., Huang, R.-J., Wang, M., Ni, H., Kampf, C. J., Cheng, Y., Bilde, M., Glasius, M., and

794 Hoffmann, T.: Molecular characterization and source identification of atmospheric particulate

795 organosulfates using ultrahigh resolution mass spectrometry, Environ. Sci. Technol., 53, 6192-6202, 2019.

796 Wang, N., Miller, C. J., Wang, P., and Waite, T. D.: Quantitative determination of trace hydrogen peroxide

797 in the presence of sulfide using the Amplex Red/horseradish peroxidase assay, Anal. Chim. Acta, 963, 61-

798 67, 2017.

799 Wang, S., Ye, J., Soong, R., Wu, B., Yu, L., Simpson, A. J., and Chan, A. W.: Relationship between

800 chemical composition and oxidative potential of secondary organic aerosol from polycyclic aromatic

801 hydrocarbons, Atmos. Chem. Phys., 18, 3987-4003, 2018b.

802   Wang, Y., Arellanes, C., Curtis, D. B., and Paulson, S. E.: Probing the source of hydrogen peroxide
803   associated with coarse mode aerosol particles in Southern California, Environ. Sci. Technol., 44, 4070-
804   4075, 2010.
805   Wang, Y., Hopke, P. K., Sun, L., Chalupa, D. C., and Utell, M. J.: Laboratory and field testing of an
806   automated atmospheric particle-bound reactive oxygen species sampling-analysis system, J. Toxicol., 2011,
807   419476, 2011a.
808   Wang, Y., Kim, H., and Paulson, S. E.: Hydrogen peroxide generation from α-and β-pinene and toluene
809   secondary organic aerosols, Atmos. Environ., 45, 3149-3156, 2011b.
810   Wang, Y., Arellanes, C., and Paulson, S. E.: Hydrogen peroxide associated with ambient fine-mode, diesel,
811   and biodiesel aerosol particles in Southern California, Aerosol Sci. Technol., 46, 394-402, 2012.
812   Wang, Y., Hu, M., Guo, S., Wang, Y., Zheng, J., Yang, Y., Zhu, W., Tang, R., Li, X., and Liu, Y.: The
813   secondary formation of organosulfates under interactions between biogenic emissions and anthropogenic
814   pollutants in summer in Beijing, Atmos. Chem. Phys., 18, 10693-10713, 2018c.
815   Wei, J., Yu, H., Wang, Y., and Verma, V.: Complexation of Iron and Copper in Ambient Particulate Matter
816   and Its Effect on the Oxidative Potential Measured in a Surrogate Lung Fluid, Environ. Sci. Technol., 53,
817   1661-1671, 2019.
818   Win, M. S., Tian, Z., Zhao, H., Xiao, K., Peng, J., Shang, Y., Wu, M., Xiu, G., Lu, S., and Yonemochi, S.:
819   Atmospheric HULIS and its ability to mediate the reactive oxygen species (ROS): A review, J. Environ.
820   Sci., 71, 13-31, 2018.
821   Xia, T., Korge, P., Weiss, J. N., Li, N., Venkatesen, M. I., Sioutas, C., and Nel, A.: Quinones and aromatic
822   chemical compounds in particulate matter induce mitochondrial dysfunction: implications for ultrafine
823   particle toxicity, Environ. Health Perspect., 112, 1347-1358, 2004.
824   Xiong, Q., Yu, H., Wang, R., Wei, J., and Verma, V.: Rethinking dithiothreitol-based particulate matter
825   oxidative potential: measuring dithiothreitol consumption versus reactive oxygen species generation,
826   Environ. Sci. Technol., 51, 6507-6514, 2017.
827   Xu, L., Guo, H., Boyd, C. M., Klein, M., Bougiatioti, A., Cerully, K. M., Hite, J. R., Isaacman-VanWertz,
828   G., Kreisberg, N. M., and Knote, C.: Effects of anthropogenic emissions on aerosol formation from isoprene
829   and monoterpenes in the southeastern United States, Proc. Natl. Acad. Sci. U.S.A., 112, 37-42, 2015.
830   Yan, D., Cui, H., Zhu, W., Talbot, A., Zhang, L. G., Sherman, J. H., and Keidar, M.: The strong cell-based
831   hydrogen peroxide generation triggered by cold atmospheric plasma, Sci. Rep., 7, 1-9, 2017.
832   Yang, R., Su, H., Qu, S., and Wang, X.: Capacity of humic substances to complex with iron at different
833   salinities in the Yangtze River estuary and East China Sea, Sci. Rep., 7, 1381, 2017.

834   Yassine, M. M., Harir, M., Dabek‑Zlotorzynska, E., and Schmitt‑Kopplin, P.: Structural characterization

835   of organic aerosol using Fourier transform ion cyclotron resonance mass spectrometry: aromaticity

836   equivalent approach, Rapid Commun. Mass Spectrom., 28, 2445-2454, 2014.

837   Yu, H., Wei, J., Cheng, Y., Subedi, K., and Verma, V.: Synergistic and antagonistic interactions among the

838   particulate matter components in generating reactive oxygen species based on the dithiothreitol assay,

839   Environ. Sci. Technol., 52, 2261-2270, 2018.

840   Zhang, Y., and Tao, S.: Global atmospheric emission inventory of polycyclic aromatic hydrocarbons (PAHs)

841   for 2004, Atmos. Environ., 43, 812-819, 2009.

842   Zhao, H., Joseph, J., Zhang, H., Karoui, H., and Kalyanaraman, B.: Synthesis and biochemical applications

843   of a solid cyclic nitrone spin trap: a relatively superior trap for detecting superoxide anions and glutathiyl

844   radicals, Free Radic. Biol. Med., 31, 599-606, 2001.

845   Zhou, J., Zotter, P., Bruns, E. A., Stefenelli, G., Bhattu, D., Brown, S., Bertrand, A., Marchand, N.,

846   Lamkaddam, H., and Slowik, J. G.: Particle-bound reactive oxygen species (PB-ROS) emissions and

847   formation pathways in residential wood smoke under different combustion and aging conditions, Atmos.

848   Chem. Phys., 18, 6985-7000, 2018.

849   Zuo, Y., and Hoigne, J.: Formation of hydrogen peroxide and depletion of oxalic acid in atmospheric water

850   by photolysis of iron(III)-oxalato complexes, Environ. Sci. Technol., 26, 1014-1022, 1992.

851

852   *Data availability*

853   The dataset for this paper is available upon request from the corresponding author (h.tong@mpic.de).

854   *Supporting Information*

855   Supporting material consists of seven figures and five tables.

856   *Author contributions*

857   HT and UP designed the esperiment and wrote up the original draft together with FL. CX, SY, and HK

858   involved in the collection of ambient particles. HT, FL, AF, and YZ particpated in laboratory measurements

859   and data analysis. All other co-authors participated in results discussion and manuscript editing.

860   *AUTHOR INFORMATION*

861   *Corresponding Author*

862   *Haijie Tong*

863   Phone (+49) 6131-305-7040

864   E-mail: h.tong@mpic.de;

865   *ORCID*:

866   Haijie Tong: 0000-0001-9887-7836

867   Maosheng Yao: 0000-0002-1442-8054

868   Thomas Berkemeier: 0000-0001-6390-6465

869   Manabu Shiraiwa: 0000-0003-2532-5373

870   Ulrich Pöschl: 0000-0003-1412-35570000-0001-9887-7836

871   *Competing interests*

872   The authors declare no competing financial interest.

873   *Acknowledgements*

880
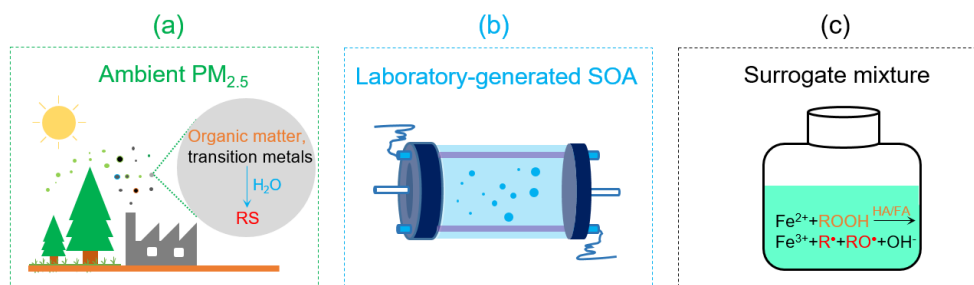
Figure 1. Schematic illustration of research approach and comparison of reactive species (RS) formed upon interaction of water with ambient fine particulate matter ($PM_{2.5}$), with laboratory generated secondary organic aerosols (SOA), and in surrogate mixtures. ROOH: organic hydroperoxide. HA: humic acid. FA: fulvic acid. $R^{\bullet}$ and $RO^{\bullet}$: C- and O-centered organic radicals, respectively.

Atmospheric
Chemistry
and Physics
Discussions

Open Access

EGU

885
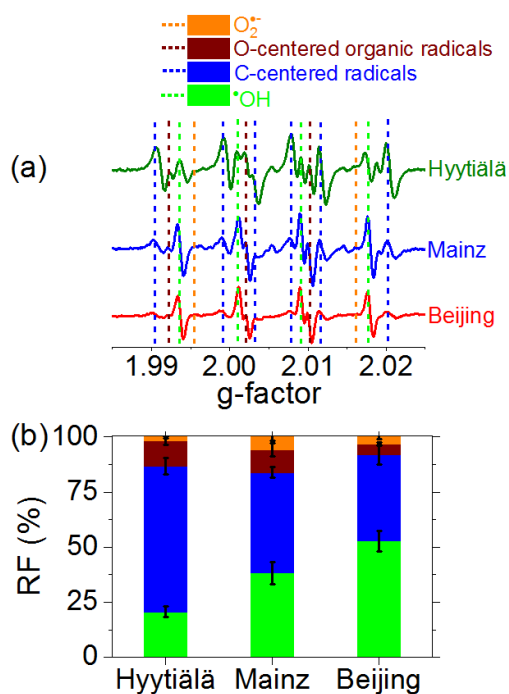
Figure 2. (a) EPR spectra and (b) relative fractions (RF) of different types of radicals formed in aqueous extracts of ambient $PM_{2.5}$ from Hyytiälä, Mainz, and Beijing. Dotted vertical lines in (a) indicate peak positions of different radical adducts. The spectra intensity in (a), RF values and error bars in (b) represent arithmetic mean values and standard error (6-13 samples per location).
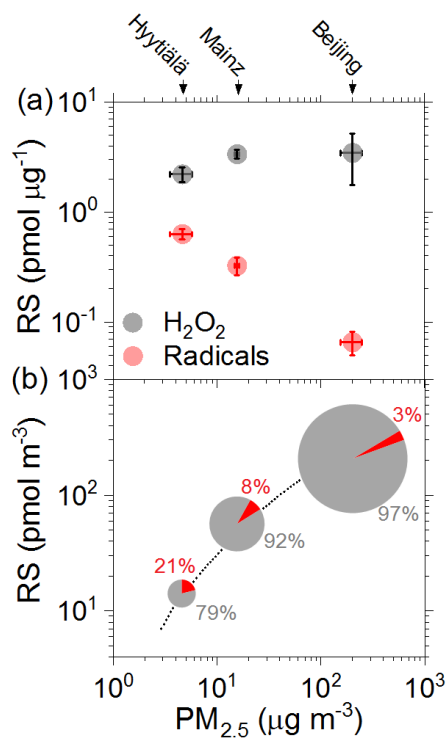
Figure 3. (a) Mass-specific yield and (b) air sample volume-specific yield of radicals (•) and H_2O_2 (•)
observed upon water interaction of fine $PM_{2.5}$ from Hyytiälä, Mainz, and Beijing plotted against $PM_{2.5}$
concentration. The error bars represent standard errors of the mean (4-12 samples per location). The dotted
line and pie charts are to guide the eye, reflecting the increase of total air sample volume-specific RS yield
(not to scale) and the relative contributions of H_2O_2 and radicals.
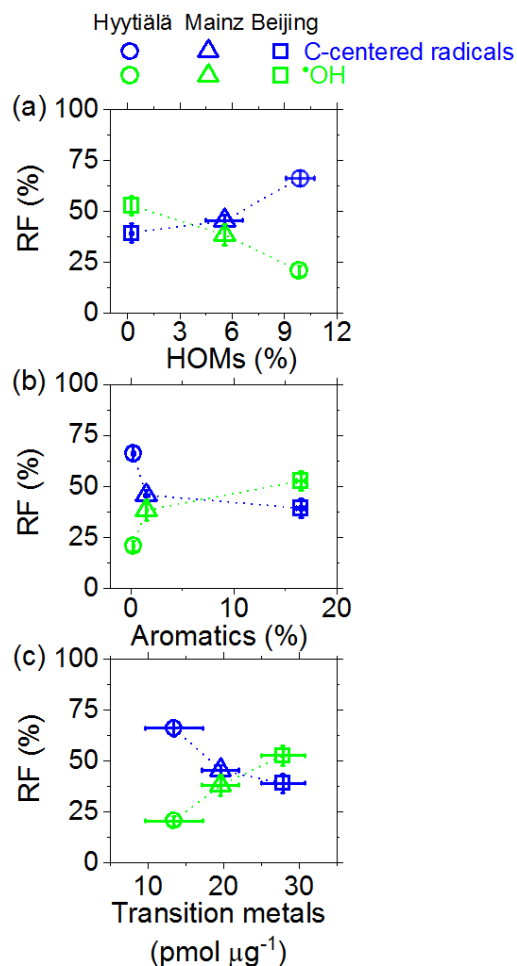
Figure 4. Correlation of (a) highly oxygenated organic molecules (HOMs), (b) aromatics, and (c) water-soluble transition metals in ambient $PM_{2.5}$ with relative fractions (RF) of $R^•$ and $^•OH$ observed upon interaction with water. The relative abundances of HOMs and aromatics in (a-b) represent the sum chromatographic area of HOMs or aromatics divided by the sum chromatographic area of all assigned organic compounds. The abundances of HOMs in (a) were adopted from a recent companion study (Tong et al., 2019). The error bars represent standard errors of the mean (4 to 12 samples per location). The dashed lines are to guide the eye.
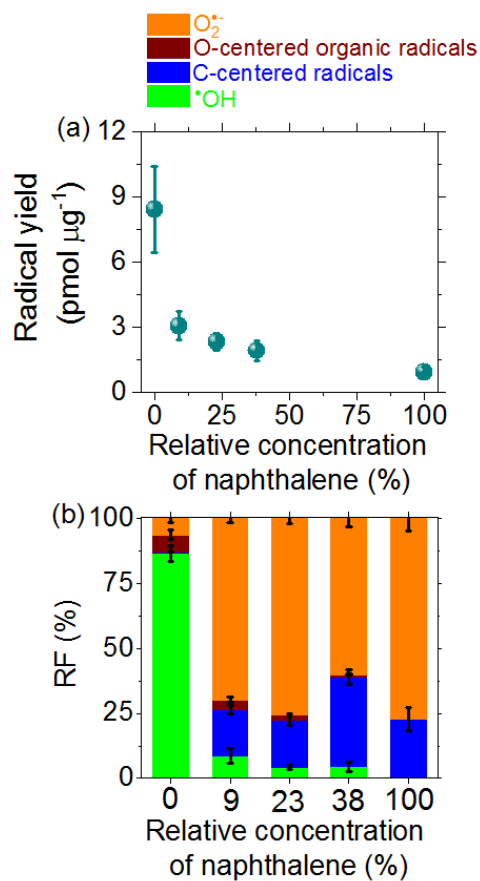
Figure 5. (a) Mass-specific yields and (b) relative fractions (RF) of radicals formed upon aqueous extraction of laboratory-generated SOA from different precursors. The relative concentration of naphthalene represents the relative molar fraction of gas-phase naphthalene to the mixture of naphthalene and β-pinene. The error bars represent standard errors (4-6 samples per data point).

909
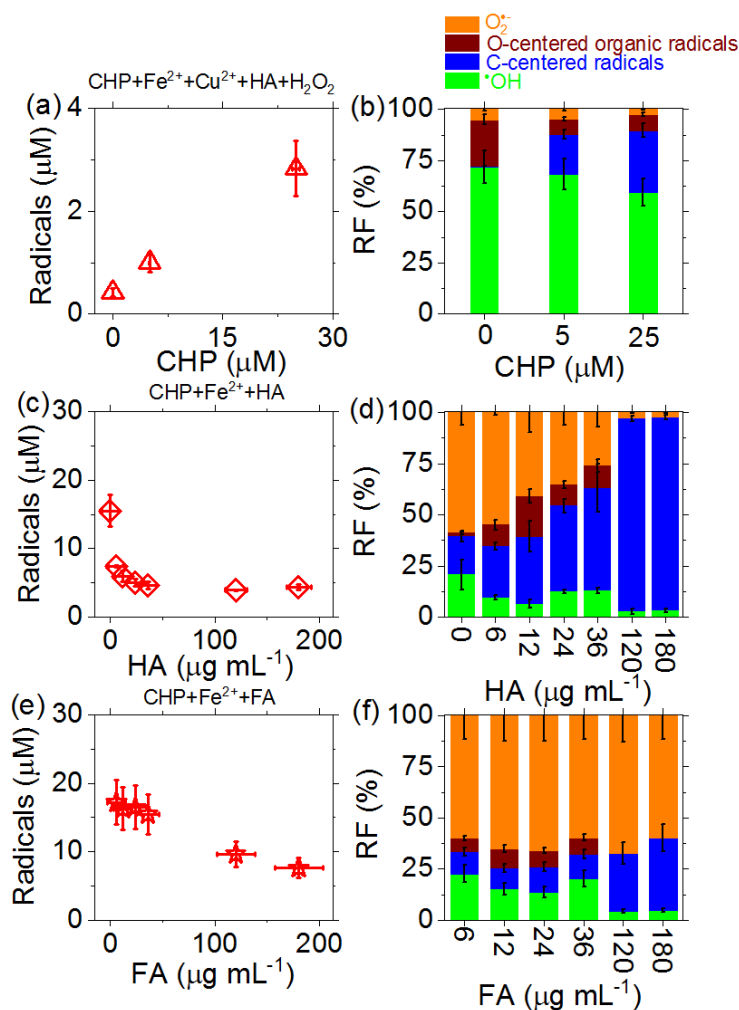
Figure 6. (a, c, e) Total radical yields and (b, d, f) relative fractions (RF) of different radical types observed in aqueous surrogate mixtures of CHP, Fe^{2+}, Cu^{2+}, HA, FA, and H_2O_2. (a, b): 0-25 µM CHP, 43 µM Fe^{2+}, 3 µM Cu^{2+}, 4 µg mL^{-1} HA, 7 µM H_2O_2 (CHP+Fe^{2+}+Cu^{2+}+HA+H_2O_2). (c, d): 100 µM CHP, 300 µM Fe^{2+}, 0-180 µg mL^{-1} HA (CHP+Fe^{2+}+HA). (e, f): 100 µM CHP, 300 µM Fe^{2+}, 6-180 µg mL^{-1} FA (CHP+Fe^{2+}+FA). The error bars represent uncertainties of signal integration of EPR spectra (for y-axis) or experimental uncertainties of the solution concentration (for x-axis). CHP: cumene hydroperoxide. HA: humic acid. FA: fulvic acid.